When did the Indus River of South-Central Asia take on its “modern” drainage configuration?

When did the Indus River take on its "modern" drainage configuration?

Yani Najman,[1] Guangsheng Zhuang,[1,2] Andy Carter[3], Lorenzo Gemignani[4,5], Ian Millar[6], Jan Wijbrans[4].

[1]LEC, Lancaster University, LA1 4YQ, UK

[2]Department of Geology and Geophysics, Louisiana State University, Baton Rouge, LA 70803, USA

[3] Dept of Earth and Planetary Sciences, Birkbeck College, University of London, UK.

[4]Institut für Geologische Wissenschaften, Freie Universität Berlin, D-12249 Berlin, Germany.

[5] Department of Earth Sciences, Vrije Universiteit Amsterdam, 1081 HV, Amsterdam, Netherlands

[6] NERC Isotope Geosciences Lab, BGS Keyworth, Nottingham, UK.

Abstract:

In order for sedimentary archives to be used as a record of hinterland evolution, the factors affecting the archive must be known. In addition to tectonics, a number of factors such as changes in climate and palaeo-drainage, as well as the degree of diagenesis, influence basin sediments. The Indus River-delta-fan system records a history of Himalayan evolution, and both the onshore and offshore sedimentary repositories have been extensively studied to research orogenesis. However, a number of unknowns remain with regards to this system. This paper seeks to elucidate the palaeodrainage of the Indus River, in particular when it took on its modern drainage configuration with respect to conjoinment of the main Himalayan (Punjabi) tributary system with the trunk Indus River. We leverage the fact that the Punjabi tributary system has a significantly different provenance signature to the main trunk Indus, draining mainly the Indian plate. Therefore, after the time when the Punjabi tributary system joined the main trunk Indus, the proportion of Indian plate material in the repositories downstream of the confluence should have a higher proportion of Indian plate material compared to the upstream repository. We

compared bulk Sr-Nd data and detrital zircon U-Pb data from the Cenozoic upstream peripheral foreland basin and downstream Indus delta and Indus Fan repositories. We determined that repositories below the confluence had a higher proportion of Indian plate material compared to repositories above the confluence, throughout Neogene times. We therefore conclude that the Indus River took on its current configuration with the Punjabi tributary system draining into the Indus trunk river in the Paleogene, early in the history of the orogen: Pinpointing the exact time when the tributary system joined the Indus should be determinable from a shift to more Indian plate input in the downstream repositories only. Whilst the upstream repository records no change in Indian plate input from Eocene to Neogene times, a shift to increased Indian plate material occurs at the Eocene-Oligocene boundary in the delta but sometime between 50-40 Ma in the fan. Further work is therefore required to understand the discrepancy between the two downstream repositories but nevertheless we can conclude that the tributary system joined the trunk Indus at or before the start of the Oligocene.

Keywords: Himalaya; Indus River; provenance; Sr-Nd analyses, zircon U-Pb analyses, mica Ar-Ar analyses.

1. Introduction

The Himalaya, as the largest orogen on Earth, garners significant interest from researchers in a variety of disciplines. Whilst considerable information on the mountain belt's evolution can be determined from its hard rock geology, its early history is often destroyed in these rocks by later tectonism, metamorphism and/or erosion. In these circumstances, researchers turn to information recorded in the sediment archive of material eroded from the mountain belt and preserved in surrounding sedimentary basins, both onshore and offshore.

48 The main repositories of Himalayan detritus are preserved in the orogen's suture zone , peripheral and
49 axial foreland basins onshore (e.g. Hodges 2000, Najman 2006, Shah 2009), and the Indus and Bengal
50 Fans offshore, which are the world's largest sediment fans (Nyberg et al., 2018). Detritus from all these
51 basins has been studied to document hinterland evolution, using a variety of bulk rock and single grain
52 analytical techniques. For example, studies of the Indus River's sedimentary repository include detrital
53 feldspar Pb isotopic analyses applied to the Indus suture zone molasse (Clift et al., 2001b), detrital zircon
54 fission track and Sm-Nd bulk analyses have been applied to the peripheral foreland basin sedimentary
55 rocks (e.g., Chirouze et al., 2015), detrital zircon U-Pb analyses have been applied to the axial foreland
56 basin (e.g., Zhuang et al., 2015) and heavy mineral and petrography (Andò et al., 2020; Garzanti et al.,
57 2020) data applied to the Indus Fan. However, in order for the sediment archives to be robustly
58 interpreted, a knowledge of the river's palaeo-drainage evolution must be known, since significant
59 drainage changes will affect the sediment archive. Reconstruction of the lower Indus palaeo-drainage is
60 the focus of this paper.

61 Today, the Indus River flows west along the Indus suture zone which separates the Indian and Asian
62 plates, before turning south across the Himalayas to flow eventually into the northern Indian Ocean,
63 giving rise to the Indus Fan (Fig. 1). Here we define the Lower Indus as that part of the Indus River
64 downstream (south) of the Himalayan mountain front, flowing axially, southward along the Indus Basin.
65 We define the Upper Indus as that part of the Indus River which flows through the mountains, sub-
66 divided into the "west-flowing axial Upper Indus" which flows from its headwaters, west, axially along
67 the Indus suture zone, and, further downstream, the "south-flowing transverse Upper Indus", which
68 cuts south across the mountain range (Fig 1A). The main tributaries to the Indus are the Punjabi or
69 Himalayan tributaries of the Jhelum, Chenab, Ravi, Beas and Sutlej Rivers, herein called the Punjabi
70 tributary system, which drain predominantly the Indian plate (Fig 1C).

Mid Eocene Owen Ridge sediments are considered to be early Indus Fan material derived from north of the Indian plate (Clift et al., 2001a; Clift et al., 2002a). This places a lower bound on the timing of initiation of the Indus River, although its upstream configuration is debated. For the Upper Indus, the proposed time of its initiation as a river flowing westward along the suture zone ranges from early Eocene through Miocene (Bhattacharya et al., 2020; Clift et al., 2001b; Henderson et al., 2011; Najman, 2006; Sinclair and Jaffey, 2001).

This paper focusses on the palaeodrainage evolution of the Lower Indus River. Various suggestions have been made regarding whether western Himalayan rivers switched between flowing east to the Ganges and Bengal Fan catchment and west to the Indus River and Fan catchment. Whilst a number of authors based their interpretations on palaeocurrent data from the peripheral foreland basin deposits (e.g. see review in Burbank et al, 1996), Clift and Blusztajn (2005) used geochemical data from the Indus Fan. They considered that changes in the geochemical signature of the Indus Fan sediment archive after 5 Ma represented a major drainage change in the Lower Indus at this time, when the Punjab tributaries to the Lower Indus River (Jhelum, Chenab, Ravi and Sutlej Rivers, Figs. 1A and 1C) switched from flowing east to the Ganges and Bengal Fan, to west to the Indus River and Indus Fan. However, Chirouze et al. (2015), considered that this geochemical change could be better interpreted as the result of variations in upland exhumation. This suggestion was later agreed upon by the original proponents of the drainage diversion hypothesis (Clift et al. (2019) and Zhou et al. (2021)) and thus the timing when the Indus River took on its current configuration with respect to the Punjab tributary system remains unknown.

Using a similar rationale to Chirouze et al (2015), we compare provenance indicators from upstream and downstream of the confluence of the Punjab tributary system with the Indus River, and from this comparison we determine when a provenance change in the downstream repository is detected and thus when the tributary system joined the trunk Indus. We extend the peripheral foreland basin Sr-Nd

dataset of Chirouze et al (2015) from the mid Miocene, down section as far as the Eocene in order to determine when the provenance change occurred, and additionally we apply new provenance indicators, namely detrital zircon U-Pb ages and detrital white mica Ar-Ar ages.

2. Background:

2.1 Himalayan geology

2.1.1 Tectonic units

The Indus suture zone separates the Asian Lhasa Terrane to the north from the Indian plate to the south. In the west, the Kohistan-Ladakh intra-oceanic island arc (KLIA) is sandwiched between the Indian and Asian plates, with the southern margin of the Asian plate at this location comprised of the Karakoram and Hindu Kush). The northern suture separating the Asian plate and KLIA is termed the Shyok Suture Zone and the southern suture separating the KLIA and Indian plate is termed the Indus Suture zone, also known as the Main Mantle Thrust in this region (Fig. 1C). The Indus River flows west along the Indus suture zone before turning south to cross the Himalaya and foreland basin before debouching into the Arabian Sea.

The Lhasa terrane comprises Phanerozoic low grade metamorphic and sedimentary cover overlying Precambrian-Cambrian basement (e.g., Leier et al., 2007). Along its southern rampart are intruded the Gangdese continental arc batholiths of the Transhimalaya which represent the Andean-type southern margin of Asia prior to consumption of the intervening Neo-Tethys ocean (Schärer et al., 1984). Whilst Gangdese intrusions are Mesozoic-Paleogene aged, post-collisional igneous activity continued into Miocene times (Hodges, 2000). To the west, the Lhasa terrane terminates against the Karakoram Fault. West of the fault, the southern margin of Asia is represented by the Karakoram (Fig 1C). The Karakoram

terrane is divided into three units (Hildebrand et al., 1998; Hildebrand et al., 2001; Searle et al., 1999): the Northern Karakoram Sedimentary Unit, the Southern Karakoram Metamorphic Belt and the intervening Karakoram Batholith. The Northern Karakoram Sedimentary Unit comprises pre-Ordovician crystalline basement covered by an Ordovician to Cretaceous sedimentary succession (Gaetani and Garzanti, 1991; Gaetani et al., 1993; Zanchi and Gaetani, 2011). The Karakoram Batholith includes pre-India–Asia collision, Andean-type subduction-related granitoids and post-India–Asia collision leucogranites. Age of metamorphism of the Southern Karakoram Metamorphic Belt ranges from Late Cretaceous to late Miocene (Fraser et al., 2001; Palin et al., 2012; Searle et al., 2010).

The Kohistan-Ladakh Island arc (KLIA) separates the Indian and Asian plates in the west of the orogen. It consists of Late Cretaceous and Eocene plutonic belts, and pyroxene granulites, calc-alkaline volcanics, amphibolites, and minor metasediments (Coward et al., 1984; Schaltegger et al., 2002), fringed by ophiolitic melange in the southern suture (DiPietro et al., 2000; DiPietro and Pogue, 2004).

The Indian plate lies to the south of the KLIA. As summarised in Hodges (2000), In the central and eastern part of the orogen, the Indian plate Himalaya is divided, from north to south, into the Tethyan Himalaya, the Greater Himalaya, Lesser Himalaya and Cenozoic foreland basin sedimentary rocks of the Sub-Himalaya (Fig 1C). Typically, the Tethyan Himalaya, separated from the Greater Himalaya to the south by the South Tibetan Detachment System, consists of Paleozoic–Mesozoic sedimentary and low-grade metasedimentary rocks which were deposited on the Tethyan ocean passive margin; the Greater Himalaya, separated from the Lesser Himalaya to the south by the Main Central Thrust, consists predominantly of medium- to high-grade Neoproterozoic-Ordovician metamorphic rocks that were subjected to metamorphism and anatexis during the Cenozoic Himalayan orogeny when they were intruded by Neogene leucogranites; and the Lesser Himalaya, separated from the Cenozoic Sub-Himalaya foreland basin sedimentary rocks to the south by the Main Boundary Thrust, consisting of

Paleoproterozoic metamorphosed and unmetamorphosed Indian plate rocks. These lithologies also broadly constitute the Indian plate Himalaya to the west in Pakistan. However, exact correlation is uncertain, the degree of metamorphism differs, and the lithologies are not structurally imbricated in the same way (Treloar et al., 2019). According to DiPietro and Pogue (2004), north of the Khairabad Thrust (MCT equivalent in Pakistan) metamorphosed rocks of ages equivalent to the Tethyan, Greater and Lesser Himalaya are found, whilst both Lesser and Tethyan equivalents are found between the Khairabad Thrust and the MBT. The Nanga Parbat syntaxis is considered to be of Lesser, Greater and Tethyan Himalayan affinity (Argles et al., 2003). In this paper, we refer to the Neoproterozoic-Ordovician rocks as *Greater Himalayan lithological correlatives*, the Paleoproterozoic rocks as *Lesser Himalayan lithological correlatives*, and the Paleozoic-Mesozoic rocks as *Tethyan Himalaya lithological correlatives*. Such terms do not reflect the location of the rocks within the various thrust-bound terranes, as they do further east.

The units described above have distinct zircon U-Pb ages and Nd isotope signatures associated with different crustal evolution histories (e.g., Argles et al., 2003; Clift et al., 2019; DeCelles et al., 2004; DeCelles et al., 2016a; Gehrels et al., 2011; Najman, 2006). These differences, (Table 1), allow for use of these techniques as provenance indicators in the detrital record downstream (e.g., Clift et al., 2019; DeCelles et al., 2004; DeCelles et al., 2016a; Gehrels et al., 2011; Najman, 2006).

The overwhelming majority of zircons from the Indian plate have U-Pb ages >400 Ma (DeCelles et al., 2004; Gehrels et al., 2011), with the minor exception of grains dated ~130 Ma from the Tethyan Himalaya (e.g. Clift et al., 2014) and Neogene grains eroded from leucogranites (e.g. Hodges, 2000 and references therein). Within the Indian plate, grains 1500-2300 Ma are characteristic of the Lesser Himalaya, and 300-1250 Ma characteristic of the Greater and Tethyan Himalaya, although not uniquely so (Clift et al., 2019). By contrast, zircons from the KLIA are exclusively aged 40-200 Ma, whilst the

southern Asian margin (the Karakoram and to the east the Lhasa Block) also have a high proportion of grains of such age, but also with some Neogene grains, and older grains stretching to the Precambrian, derived from the substrate into which the Mesozoic-Paleogene plutons intruded (e.g. Zhuang et al., 2018 and references therein).

The old continental crust of the Indian plate has a mean ε_{Nd} value of -15 for the Greater Himalaya, -22 for the Lesser Himalaya, and -11 for the Tethyan Himalaya (Ahmad et al., 2000; Deniel et al., 1987; Richards et al., 2005; Robinson et al., 2001; Zhang et al., 2004). By contrast, the Asian and intra-oceanic arc terranes have more positive values, reflecting the dominance of Mesozoic-Paleogene plutons: the KLIA has values around +5 (Bignold and Treloar, 2003; Khan et al., 1997; Khan et al., 2004; Khan et al., 2009), whilst the Karakoram, which consists of both old sedimentary and metamorphic rocks as well as younger plutons, has an average value around -9.6 (Mahéo et al., 2009; Miller et al., 1999). Data from the Lhasa Block are mainly from the central and eastern part of the orogen: the Gangdese / Transhimalaya have values ranging from +0.9 to 5.5 for the Mesozoic granitoids and +2.4-8.5 for the Paleocene-Eocene granitoids in contrast to the Oligocene-Miocene granitoids with values of -9.4 to 5.5 (Ji et al., 2009; Pan et al., 2014), whilst the continental substrate into which these plutons intruded have an average recorded ε_{Nd} value of -9 (Pan et al., 2014; Zhu et al., 2009; Zhu et al., 2012).

2.1.2. Tectonic evolution.

Prior to India-Asia collision, India was subducting beneath Asia as Neo-Tethys closed, with the KLIA located between the two continents in the west. The timing of India-Asia collision, and whether the island arc collided with India or Asia first, is disputed; a majority of researchers consider India-Asia collision occurred around 55-60 Ma (see review in Hu et al., 2016 and references therein) with other estimates extending to c. 35 Ma or 25-20 Ma (Aitchison et al., 2007; Bouilhol et al., 2013; van Hinsbergen et al., 2012).

The west differs from the better studied east and central part of the orogen in both the presence of the KLIA, and in the timing of exhumation of the Indian plate. In the west, a tectonic wedge consisting of the KLIA, ophiolitic melange and thrust slices of Lesser Himalayan and Tethyan correlatives of the Indian plate was in position and thrust over the Indian plate foreland prior to 47 Ma. Thereafter, Indian plate Lesser-, Greater- and Tethyan Himalayan correlatives were exhumed from beneath the wedge (DiPietro et al., 2008), predominantly during the Paleogene with a pulse of deformation also in the earliest Miocene, ~20 Ma (Argles et al., 2003, and references therein; DiPietro et al., 2021). Substantial rapid exhumation of the Indian plate hinterland is not recorded after this time, except in the Nanga Parbat region (Fig 1C), a syntaxis of Lesser, Greater and Tethyan Himalayan lithological correlatives, where rapidly accelerating exhumation is recorded over the Pliocene (e.g., Schneider et al., 2001). Thrusting and exhumation propagated south towards the foreland in the mid or late Miocene, continuing into the Pliocene (Burbank and Tahirkheli, 1985; Yeats and Hussain, 1987).

To the north of the Indian plate, moderate exhumation is recorded from Eocene times in the Kohistan Island arc (Van Der Beek et al., 2009) and by contrast, the Karakoram of the Asian plate records periods of rapid exhumation around 27-35 Ma, 13-17 Ma, 7-8 Ma and 3.3-7.4 Ma (Dunlap et al., 1998; Wallis et al., 2016; Zhuang et al., 2018).

2.2. Foreland basin geology

In Pakistan, current basinal environments along which the modern Indus River flows, consist of (1) the peripheral foreland basin that strikes east-west along the southern margin of the orogen, and (2) the north-south striking Lower Indus axial foreland basin along which the Lower Indus River debouches into its delta in the Arabian Sea (Fig. 1A).

2.2.1 Peripheral foreland basin

Foreland basin stratigraphy is for the most part invariant along strike in the orogen, with local minor facies variation, although formation names differ. In Pakistan, the Paleogene has a number of formation names for equivalent units, in different areas (Pivnik and Wells, 1996). We adopt the formation names in our area of study, which for our Paleogene samples is the Hazara-Kashmir syntaxis (HKS) (Figs. 1A and B), with the stratigraphy as recorded in Table 1. At this location, the Paleocene Lockhart Limestone is overlain successively by the latest Paleocene (57-55 Ma) Patala Formation, the early Eocene (55-53 Ma) Margala Hill and Chorgali Formations, and the early-Mid Eocene (53-43 Ma) Kuldana Formation (Baig and Munir, 2007; Bossart and Ottiger, 1989; Ding et al., 2016b; Qasim et al., 2018). These formations, which stretch from marine facies to the transitional Kuldana Formation, are separated from the overlying continental alluvial facies by a late Eocene-Oligocene unconformity. Above the unconformity, there is the Murree Formation, also called the Balakot Formation in the HKS. In this syntaxis, the Murree Formation has a latest Oligocene maximum depositional age (MDA) as determined by the two youngest zircons within error, with a weighted mean U-Pb age of 22.6 ± 1.0 Ma (this study, section 4.2) from a sample collected near Paras, north of Balakot (Fig. 1B), supported by a grain dated at 22.7 +/- 0.4 Ma (Ding et al 2016b) from a section 15 kms south at Muzaffarabad (Fig. 1B). South-west of the Hazara-Kashmir syntaxis, at Murree hill station (MHS) (Fig. 1B), detrital mica Ar-Ar ages indicate an MDA of <24 Ma (this study, section 4.3). These MDAs are in agreement with the early Miocene dating of the Murree Formation to the south, based on mammal fossils (Shah, 2009). Further south, in the Kohat and Potwar Plateaus (Fig. 1A) are the alluvial Kamlial Formation and overlying Siwalik Group, subdivided into the Chinji, Nagri and Dhok Pathan Formations (see Table 1 for stratigraphy). These formations are dated by magnetostratigraphy (Johnson et al., 1985), at 18-14 Ma, 14-11 Ma, 11-8.5 Ma, and <8.5 Ma, respectively.

2.2.2 Lower Indus axial Basin

The stratigraphy of the Lower Indus Basin in the Sulaiman and Kirthar regions are broadly correlative (Shah, 2009). It encompasses the early Eocene Ghazij Formation, the middle-late Eocene Kirthar Group, the Oligocene-early Miocene Chitarwata Formation, the late Early to middle Miocene Vihowa Formation, and the middle Miocene-Pliocene rocks of the Siwalik Group (Roddaz et al., 2011; Shah, 2009; Zhuang et al., 2015), as denoted in Table 1. Facies are predominantly marine until the Chitarwata Formation which transitions up from deltaic to fluvial facies. Fluvial facies then persist until the top of the section.

2.3 Paleodrainage models

2.3.1 The early drainage configuration of the palaeo-Indus: evidence from the Indus Fan sedimentary archive

The oldest eastern Indus Fan sample (IODP 355, U1456 and 1457, Fig 1A) to have been subject to detrital zircon U-Pb analyses is 15 Ma. This shows evidence of input from the Karakoram (Zhou et al., 2022), indicating the drainage basin of the palaeo-Indus stretched as far back as the Shyok Suture Zone by this time (Fig 1C). The oldest sample subjected to detrital zircon U-Pb dating in the western part of the Indus Fan (ODP 731, Fig 1A) is ~ 30 Ma. This sample shows evidence of input from the KLIA/Asian plate (undifferentiated), indicating that the river stretched back at least beyond the Indus Suture Zone (Fig 1C) by that time (Feng et al., 2021). Likewise, Mid Eocene Owen Ridge sediments from DSDP 224 (Fig 1A), considered to be early Indus Fan deposits (Clift et al., 2001a; Clift et al., 2002a), show bulk rock ε_{Nd} signatures and K-feldspars with Pb isotope compositions indicative of derivation from north of the Indian plate (Clift et al., 2001a). This indicates that the river's drainage basin stretched back as least as far as the Indus Suture Zone and KLIA at this time.

2.3.2. The early drainage configuration of the upper axial palaeo-Indus: evidence from the Indus Suture Zone molasse.

Clift et al. (2001b) considered that various isotopic provenance datasets and palaeocurrents in Indus suture zone sedimentary rocks of early Eocene age indicated contribution from the Lhasa Block to the east, requiring along strike east to west flow along the suture zone at that time. However, Najman (2006) argued that an alternative source with a suitable signature could potentially be that of the Karakoram, located north of the suture zone sediments under discussion, and therefore not requiring along-strike transport and axial flow. Sinclair and Jaffey (2001) considered their facies analyses of the suture zone sediments indicated internal rather than through-flowing drainage until at least the early Miocene. Later, Henderson et al. (2010) reported that white micas, interpreted as Indian-plate derived, first occurred in the same suture sedimentary rocks as Asian-derived zircons, in suture zone sedimentary rocks dated <23 Ma. From these mixed source sedimentary rocks, and accompanying facies analysis, they considered the Indus River was flowing in the suture zone at that time. However, it should be noted that (1) micas were also recorded in older suture zone sedimentary rocks but they were of too small grain size to analyse, (2) Indian plate material with low muscovite fertility such as from the Tethyan Himalaya may well have contributed to the suture zone rocks earlier and (3) an open question remains as to why the first appearance of micas interpreted as Indian-derived, was not also accompanied by an influx of Paleozoic and older zircons, also typical of the Indian plate. Whilst subsequently, such old zircons, interpreted as Indian rather than Asian-derived, have been documented in suture zone sediments as old as ca. 50 Ma (Bhattacharya et al., 2020), nevertheless they are not present in the samples analysed for white mica Ar-Ar analyses by Henderson et al (2010). Whilst mineral sorting due to different hydraulic regimes of zircon versus mica (Malusà et al., 2016) might explain the difference, we suggest that, with the benefit of subsequent better characterisation of the ages of micas from the southern margin of the Asian plate (Zhuang et al 2018), an Asian Karakoram provenance might provide an alternative provenance for these micas. Regardless, mixed Indian-Asian provenance, unaccompanied by facies data indicating deposition in a major river, does not indicate east-west through-flow of

drainage. Bhattacharya et al. (2020) demonstrated from provenance data that detritus from the east was transported west by ca 27 Ma. Thus we may conclude that an axial upper Indus flowed west by Oligocene times. Prior to that the suture zone was a depocentre, but it may have been externally or internally drained.

2.3.3. Early drainage configuration of the upper transverse palaeo-Indus River: evidence from the peripheral foreland basin deposits

In the peripheral foreland basin, detrital blue-green hornblende considered to be derived from the KLIA, is first recorded in the Kohat and Potwar plateaus from 11 Ma (Nagri Formation), interpreted as palaeo-Indus deposits (Abbasi and Friend, 1989; Cerveny and Johnson, 1989). Ullah et al. (2015) applied geochemistry and petrography to the Chinji Formation (14-11 Ma) to record material from the KLIA and Indus suture zone. Based on petrography, Najman et al. (2003) recorded arc-derived detritus in the Potwar plateau from the start of their studied section at 18 Ma, from which they interpreted that this time represented the first arrival of sediment from the Upper Indus River to the foreland basin in this region. Still later work (Ding et al., 2016b; Qasim et al., 2018) recorded arc-derived zircons in the foreland basin latest Paleocene to Early Eocene Margala Hill and uppermost Patala Formations, indicating derivation from north of the Indus Suture Zone / Main Mantle Thrust since at least 55 Ma.

Whilst the above provenance data indicates derivation from material as far north as the KLIA since Eocene times, whether these rocks represent the deposits of the palaeo-Indus is debated (Cerveny et al., 1989; Willis, 1993; Zaleha, 1997). Chirouze et al (2015) proposed a Lhasa Block origin for detrital zircons with old fission track ages in the Chinji Formation. This would indicate that the contributing drainage basin stretched into the Shyok Suture Zone and Asian plate by this time, and was therefore likely the palaeo-Indus. However, we suggest that such grains may also be derived from the Indian Himalayan units south of the KLIA, as arguable by their occurrence in the Siwalik foreland basin

sedimentary rocks of Nepal, that were deposited by rivers which did not stretch back to Asia (Bernet et al., 2006).

However, more definitive evidence of deposition from the palaeo-Indus comes from detrital mica Ar-Ar data. Lag times of detrital mica Ar-Ar ages from Kamlial Formation Potwar Plateau sedimentary rocks indicate rapid exhumation of the upland source region from 16-14 Ma (Najman et al., 2003). The exhuming source area was interpreted by those authors to be the Karakoram and/or Nanga Parbat region, consistent with both bedrock data from those regions (Treloar et al., 2000; Zhuang et al., 2018 and references therein). Due to their locations, derivation of micas from either location strongly suggests transport by a palaeo-Indus. Furthermore, detritus delivered by possible ancient smaller tributaries draining only the Indian plate and arc would have had a distinct and different signature, with a higher proportion of Indian plate detritus, for example the Mid Miocene Kamlial Formation sample CP96-6A from Najman et al. (2003), and presumably those samples from the Eocene Kuldana Formation with a high proportion of old zircons at Muzaffarabad (Ding et al., 2016b) (see section 5.2 for further discussion).

2.3.4. Evolution of the Lower Indus palaeodrainage

Within the basin, the position of the Ganges-Indus drainage divide over time is long debated, with various authors proposing that parts of the current Gangetic catchment used to flow into the Indus Fan (e.g. DeCelles et al., 1998), and the current Indus River catchment into the Bengal Fan (e.g. Burbank et al., 1996) at various times. Clift and Blusztajn (2005) noted a change to more negative ε_{Nd} values in the Indus Fan at 5 Ma, which they interpreted as the drainage diversion of the major Indian-plate draining Punjabi Indus River tributary system of the Jhelum, Chenab, Ravi and Sutlej rivers (Figs. 1A and C) from a previous routing towards the Ganges and the Bengal Fan to the east.

However, the above argument was countered by Chirouze et al. (2015) who looked at both spatial and temporal trends at the range front and Indus Fan. They considered that the change in the signal was due to differential exhumation in the hinterland rather than drainage re-organization. They compared ε_{Nd} data between the range front and Indus Fan for both the present day and the Miocene (using Chinji Formation foreland basin data for the Miocene range front). They recorded a spatial variation of four ε_{Nd} units between the range front and the Indus Fan for both mid-late Miocene times and modern day (Miocene range front and Indus Fan values at -6 and -10 respectively; modern day range front and Indus Fan values at -10 and -14 respectively. This suggests a stable drainage pattern for the lower Indus since at least the mid-late Miocene. From the above data they noted a negative shift of ~3 ε_{Nd} units between Miocene and the modern day at both the range front (comparison of Miocene foreland basin sedimentary rocks with modern day Upper Indus values) and a similar shift in the Indus Fan. From this temporal shift they therefore concluded that the variation over time was due to the changing exhumation rates of the contributing source regions, with the exhumation and thus contribution of the Karakoram / Indian plate syntaxial Himalaya increasing at the expense of the more positive KLIA (Table 1) to explain the shift in ε_{Nd} values in the Indus Fan at 5 Ma. They supported their proposal of variations in exhumation using detrital zircon fission track (ZFT) data, interpreting a decrease in older ZFT ages after 12 Ma as due to decreased input from the KLIA. Later, the original proponents of the drainage capture hypothesis (Clift and Blusztajn, 2005) concurred with the view of Chirouze et al. (2015) that changes in the tectonics of the hinterland was the more likely cause of the geochemical change in the Indus Fan at 6 Ma (Clift et al., 2019; Zhou et al., 2022) thus the time when the Punjab tributary system joined the trunk Indus remains unknown. It is towards this question, namely the evolution of the downstream Indus, that this paper focusses.

The location of the exit of the Indus River to the ocean in the past retains a level of uncertainty. Today the Indus River debouches to the Arabian sea at the south of the Lower Indus axial Basin. These deposits

346 are recorded in eastern Sulaiman and Kirthar regions of the Lower Indus Axial Basin (Welcomme et al.,
347 2001) (Fig 1A). Zhuang et al. (2015) show that zircons from the KLIA are recorded in these sediments
348 from at least early Oligocene times; they considered that detrital zircon U-Pb data indicate input from
349 the Karakoram from at least Mid Miocene times, and that Sr-Nd data indicate a palaeo-Indus origin from
350 50 Ma. Roddaz et al. (2011) carried out mixture modelling on their Sr-Nd data and concluded that there
351 was an appreciable input from the Karakoram since 50 Ma.

352 However, Palaeogene deltaic facies have also been identified in the Katawaz remnant ocean Basin (Fig
353 1A) to the west (Qayyum et al., 2001). In view of the differing compositions and provenance between
354 these two deltaic systems, Roddaz et al. (2011) proposed two river-delta-fan systems, with the Katawaz
355 system debouching into the Khojak submarine fan and the sediments of the Lower Indus Axial Basin
356 debouching into the Indus Fan. Provenance data from the Katawaz rocks show that that drainage basin
357 stretched back at least as far as the KLIA by Miocene times (Carter et al, 2010) with a paucity of data
358 currently precluding earlier documentation. For a full evaluation of the Indus river-delta-fan system and
359 the spatial evolution, more data are needed from the Katawaz basin; data presented in this paper
360 provide a direct comparison between peripheral foreland basin records and terminal sinks in the delta
361 and ocean.

362

363 **3. Methods**

364 ***3.1 Rationale and approach***

365 To determine when the Punjab tributary system joined the trunk Indus, we leverage that fact that the
366 tributaries have a very different drainage basin lithology to the trunk Indus; the former includes only
367 Himalayan units, whilst the drainage basin of the latter includes also the KLIA and Asian plate (Fig. 1C),
368 which have very different isotopic and geochemical signatures to the Indian plate (Table 1). This

difference is clearly reflected in both the Sm-Nd and zircon U-Pb characteristics of the trunk Indus river versus the Punjabi tributary system: Figs 2and 3A (inset) shows that, compared to the modern Indus trunk river, the Punjabi tributaries have a more negative εNd value and a much lower proportion of young arc-aged grains (Alizai et al. 2011, Chirouze et al 2015), a signature which extended back into the ancient sedimentary record (Exnicios et al., 2022; Najman et al., 2009).

We took a similar approach to Chirouze et al (2015) in hypothesising that prior to the time when the Punjab tributary system joined the trunk Indus River, the sedimentary repositories upstream and downstream of the confluence should look similar in terms of provenance. After the time when the tributary system joined the Indus River, the repository upstream of the confluence should remain similar (unless synchronously affected by a tectonic-induced change in the hinterland), but the downstream repository should show increased input from Himalayan Indian plate units.

We therefore made comparison between data upstream (our new foreland basin data) and published data downstream of the Punjab tributary system. Previous work used the Indus Fan as the downstream comparative repository. We use both the deltaic record in the Sulaiman and Kirthar region, and the Indus Fan archive, since onshore sedimentary archives are typically more prone to diagenetic alteration compared to marine records, whilst distal deposits are more prone to the effects of hydraulic sorting (e.g., Garzanti et al., 2020) and contain evidence of subordinate extraneous (non-Indus River) sources to the Himalayan orogen, such as the Deccan Traps of peninsular India input to the Indus Fan (Clift et al., 2019; Garzanti et al., 2020; Yu et al., 2019). The Indus Fan record is a composite repository of material recovered from the Owen Ridge and Western Fan from DSDP 224 (Eocene-Miocene) and ODP 720, 722 and 731 (Eocene-Pleistocene) sites, and IODP 355 sites of U1456 and1457 of the Eastern Fan (Neogene only) (Clift et al., 2019; Feng et al., 2021; Zhou et al., 2022) (Fig. 1A).

Our dataset builds on the previous work of Chirouze et al. (2015) in two ways. Firstly, it expands the time range from the previous mid Miocene study of the Pakistan peripheral foreland basin to now include foreland basin rocks from Eocene to late Miocene. This allows a more complete assessment of the evolution of the lower Indus to be determined. Secondly, we incorporate not only ε_{Nd} data from mudstones, but also new and previously published zircon U-Pb data to assess provenance, and mica $^{40}Ar/^{39}Ar$ data to assess exhumation. Therefore, in addition to using both onshore and offshore repositories to limit the potential effects of fertility, diagenetic, and hydraulic sorting biases, our multi-proxy approach provides additional mitigation since: 1) zircons are resistant to diagenesis; 2) we assess evidence from both the mud and sand grain size fractions with the use of both bulk and single grain approaches and 3) we obtain data from both zircon and mica grains which respond differently to the hydraulic regime (e.g., Garzanti and Andò, 2019; Garzanti et al., 2009; Malusà et al., 2016). Furthermore, since white mica is rare in the KLIA, exhumation patterns of the Karakoram and Indian plate Himalaya can be considered in isolation using this technique, unbiased by potential issues surrounding dilution and fertility.

3.2. Samples and analyses

3.2.1 Samples

We analysed 5 sandstones for detrital zircon, 10 mudstones for Sr-Nd isotopes, and 3 sandstones for mica $^{40}Ar/^{39}Ar$. The locations of analysed samples (Figs. 1A and B) are from the Kuldana Formation in the HKS at Paras north of Balakot, the Murree Formation in both the HKS and at Murree Hill Station (MHS), and the Kamlial, Chinji and Nagri Formations from the Chinji section on the Potwar Plateau, the latter being the same location from which Chirouze et al (2015) took their samples. A summary of our sample information is tabulated in S1. Our samples from the Kuldana Formation are structurally imbricated within the Murree Formation (Najman et al., 2002). Originally, Najman et al (2002) considered these

structural imbrications to be Patala Formation, based on the work of Bossart and Ottiger (1989) who did not recognise the Kuldana Formation. However, more recent detailed mapping (Ding et al., 2016b) and the better agreement of biostratigraphic ages from the structural imbricates (early-mid Eocene; Bossart and Ottiger (1989)) with the Kuldana Formation rather than Patala Formation (section 2.2.1), suggests reassignment of these imbricates from the Patala to the Kuldana Formation.

3.2.2 Sr-Nd bulk analyses

Sr and Nd isotope analyses on bulk mudstones were carried out at the NERC Isotope Geosciences Laboratory, Keyworth, Nottingham. Samples were leached in dilute acetic acid in order to remove carbonate material, then dissolved using HF-HNO3 and converted to chloride form. Sr and a bulk REE fraction were separated using AG50x8 cation columns, and Nd was separated from the bulk REE using LN-SPEC columns. Sr and Nd were analysed on a Thermo Scientific Triton mass spectrometer.

3.2.3 Zircon U-Pb analyses

Detrital zircon U-Pb ages were acquired using laser ablation ICPMS, at the London Geochronology Centre, University College London. To avoid bias, polished grain mounts were made, without hand picking, directly from Diidomethane sink fractions with a grain size ≤ 300 µm. Each laser spot (25 µm) was placed on the outermost parts of each grain to target the youngest growth stage. Between 150-320 grains were analysed for each sample, providing statistical confidence of detecting all component ages. Data were processed using GLITTER v4.4 data reduction software using age standard bracketing to correct for mass fractionation. Between 8 and 15% of ages were rejected, due to high discordance from lead loss, zoning or mixing of growth zones. One exception was the Chinji Formation that contained an unusually high number (60%) of discordant grains. Most of these discordant grains are associated with ages between 75-120 Ma and consistent with lead loss, likely due to source weathering.

3.2.4 Muscovite Ar-Ar analyses

Muscovite Ar-Ar ages were analysed at the Argon Geochronology Laboratory at VU University Amsterdam, Netherlands. Individual grains ranging from 125-1000 μm were handpicked under a binocular microscope to avoid obvious weathering or inclusions. After irradiation at the Oregon State University TRIGA nuclear reactor, total fusion analyses were carried out with a ThermoFisher Scientific Helix MC plus multi-collector mass spectrometer, fitted with 10^{13} Ohm amplifiers. Data reduction was done using ArArCALC2.5 (Koppers, 2002).

Detailed methodologies are provided in SI 1, and results are reported in Tables S1 (Sr-Nd data), S2 (zircon U-Pb data) and S3 (mica Ar-Ar data).

4. Results and integration with published data

4.1 Sr/Nd bulk (Figs. 2 and SI Fig S1, Table S1)

There is little significant variation in ε_{Nd} values from the Eocene Kuldana Formation through to the late Miocene Nagri Formation, with values ranging between -7.0 to -9.2 (Fig. 2A). The exception to this overall similarity is the Murree Formation at MHS, with a value of -13.8. We note that previous work for the Chinji Formation records values of -3.8 to -7.7 (Chirouze et al., 2015); this difference could perhaps reflect the previous use of sand compared to analysis of muds in the current research (see Jonell et al., 2018 for further discussion). There are no modern-day data available for the range front. The Upper Indus has a value of -10.8 at Besham (Clift et al., 2002b) located just downstream of the Kohistan arc (Fig. 1B and C) and we can extrapolate that values should be more negative than this at the range front, after the river has passed over the Greater and Lesser Himalaya. Values at the delta front at Thatta are -14.9 (Clift et al., 2002b).

We carried out mixture modelling on the foreland basin material (SI Fig. S1). The mixture modelling is complicated by the number of end member contributors; today sediment in the Upper Indus River contains material from the Lhasa Block, Karakoram, KLIA, suture zone, and the Indian plate units of the Greater-, Lesser- and Tethyan Himalayan correlatives. Overlapping signatures of some units (e.g. between the Karakoram and Tethyan Himalaya, and between the KLIA and ophiolitic melange of the suture zone) also adds uncertainty. We started with the premise that, from the zircon data we are confident that the foreland basin contains material from the KLIA (section 4.2.) from the oldest sediments studied, namely the early-Mid Eocene Kuldana Formation. That therefore forms the apex of our model, and various mixture couplings are calculated with this apex and other potential end members. The modelling shows that all data can be explained by a mix of Indian plate and KLIA inputs, and contribution from the Karakoram and Lhasa Block is equivocal. The Murree Formation sample from MHS requires considerable input from Greater Himalayan lithological correlatives.

The Sr-Nd compositions of the samples plot on trends that are consistent with simple mixing between mafic and more evolved sources. There is some scatter in the data towards high Sr^{87}/Sr^{86} values that may result from weathering or diagenesis. However, we are confident that the dominant trends reflect changes in provenance, as described above.

4. 2 Detrital zircon U-Pb analyses (Fig 3, SI Figs S2 and S3, Table S2)

We compile our new data from the Murree Formation at Paras north of Balakot in the HKS and at MHS (< 24 Ma), and from the Kamlial (18-14 Ma), Chinji (14-11 Ma) and Nagri (11-8.5 Ma) Formations in the Potwar Plateau, with previously published data from the Kuldana and Murree Formation rocks at Balakot, Muzaffarabad and Kotli in the HKS and at MHS (Awais et al., 2021; Ding et al., 2016a; Qasim et al., 2018) and modern river data collected at the MCT-correlative (Khairabad Thrust) at the range front at Attock (Alizai et al 2011, Clift et al 2022) (Fig. 1B). We keep our observations of comparisons broad

and conservative in nature, since different approaches to both mineral separation and data processing procedures by different labs can cause variation in proportions of different populations. We begin our summary at the marine to continental transition (the Kuldana Formation, section 2.2.1). We focus on the 40-200 Ma "arc-aged" population characteristic of the KLIA and Karakoram, and the older grains typical of the Indian plate and Karakoram, with emphasis on the 1500-2300 Ma population typical of the Lesser Himalayan lithological correlatives and 300-1250 Ma population typical of the Greater Himalayan lithological correlatives (section 2.1.1, Table 1).

With the exception of the Murree Formation (which we portray separately in Fig 3B and discuss separately in section 5.2), the proportions of the 40-200 Ma "arc-aged" populations remain approaching or above 50% throughout the Neogene to present day. There is much variation within the Eocene Kuldana Formation, with nevertheless a number of samples also showing a majority of grains to be arc aged (Fig. 3A, Table 1). By contrast, the Murree Formation has a very low proportion of grains in the 40-200 Ma range in all samples analysed from MHS, Muzaffarabad and Balakot, although not at Paras north of Balakot in the HKS (Fig 1B, Fig 3B and SI Fig S2). Instead, these Murree Formation samples from MHS, Muazaffarabad and Balakot have a high proportion of grains with ages typical of the Greater Himalaya. In contrast to the modern-day river sample at Attock (Fig. 3C, Fig 1B), there is no 1500-2300 Ma population typical of the Lesser Himalayan lithological correlatives, in any of the formations.

4.3 Mica Ar-Ar (Fig 4, SI Fig. S4, Table S3)

We have integrated our new data from the Murree Formation at MHS, Chinji and Nagri Formations with previous data from the Murree Formation in the HKS at Paras north of Balakot (Najman et al., 2001) and Kamlial Formation (Najman et al., 2003) (SI Fig. SI4). We note the following, bearing in mind that the number of grains analysed for the Murree Formation at Paras north of Balakot (n=257) and the Kamlial Formation (n=277) are considerably higher than for the Murree Formation at MHS, Chinji and Nagri

samples (n=59, 94 and 43 respectively), resulting in more confidence that the Balakot and Kamlial Formation datasets more completely capture the complete spectrum of ages:

The youngest grain in the Murree Formation at Paras in the HKS is 24.6 +/- 0.7 Ma, the weighted mean of the youngest two grains overlapping within error at two sigmas is 24.8 Ma +/- 1.4 Ma and the youngest peak population is 37 Ma. Pre-Cenozoic ages extend to >1500 Ma. Further south, the youngest grain in the Murree Formation at MHS is 23.7 +/- 0.1 Ma, which also forms one of the two youngest grains overlapping within error at 2 sigmas (weighted mean 23.85 +/- 0.12 Ma. The youngest peak population is 24-28 Ma. Pre-Cenozoic ages extend to ca 450 Ma. The youngest grain for the Kamlial Formation is 14.5 +/- 0.7 Ma, and weighted mean of the youngest two grains within error at 2 sigmas is 15.00 +/- 1.10a. The youngest peak population is 18 Ma and Pre-Cenozoic ages extend to ca 450 Ma. The lowest Chinji Formation sample (CP96-7A, Najman et al 2003, dated at 13.9 Ma) has a youngest grain at 14.1 +/- 0.7 Ma and this also forms one of the two youngest grains within error at 2 sigmas (weighted mean 14.43 +/- 0.81 Ma). Pre-Cenozoic grains extend to 400 Ma. Our new sample from the Chinji Formation has a youngest grain of 16.74 +/- 0.1 Ma, the weighted mean of the two youngest grains overlapping within error at 2 sigmas is 25.95 +/0 0.10 Ma, the youngest peak population is 28-29 Ma, and Pre-Cenozoic ages extend to ca 450 Ma. The youngest grain in the Nagri Formation is 17.9 +/- 0.14 Ma, the weighted mean of the two youngest two grains overlapping within error at 2 sigmas is 19.69 +/- 0.12 Mathe youngest peak population is 21 Ma and Pre-Cenozoic ages extend to ca 200 Ma.

Rapid exhumation determined from short lag times was determined for the Kamlial and lowest Chinji Formation, between 16-14 Ma (Najman et al, 2003) (Fig. 4). Lack of independent depositional age constraints precludes calculation of lag times for the newly analysed Murree, Chinji and Nagri Formation samples. Up section from the Kamlial Formation, there is no evidence of grain ages approaching

depositional age, until the modern river sample at Thatta, although the number of grains analysed is relatively small.

5. Interpretations of the evolution of the Lower Indus drainage

5.1. When did the Punjabi tributary system join the paleo-Indus trunk river?

As outlined in our rationale and approach (section 3.1), we determine when the Punjab tributary system joined the main trunk river, by a comparison of provenance data from upstream and downstream of the present day confluence, leveraging the fact that unlike the palaeo-Indus trunk River, the tributaries drain only the Indian plate terranes (Fig 1C), and thus have a different provenance signature (section 3.1, Figs 2 and 3A inset).

As schematically presented in Fig 5, the following evidence should be met, at the time the tributary system joined the trunk Indus:

(1) Prior to the time that the Punjab tributary system joined the Indus catchment, the proportion of Indian plate detritus delivered to the Indus River should be comparable at the range front and at the river mouth, i.e. upstream and downstream of where the Punjab tributary system now joins the modern Indus.

(2) After the time when the Punjab tributary system joined the Indus River, the proportion of Indian plate material in the Indus River downstream of the confluence with the Punjab Rivers should a) increase relative to the downstream's previous pre-reorganisation proportion and b) be greater than coeval sediments upstream. However, the proportion of Indian plate material in the upstream should remain constant, pre and post the proposed drainage reorganisation.

For the above predictions to be explored, Indian plate, versus Karakoram, versus KLIA must be differentiable in the foreland basin detritus. Table 1 provides the typical zircon U-Pb and ε_{Nd} signatures of these units, alongside a summary of equivalent data from the peripheral foreland basin, and downstream in both the Sulaiman-Kirthar region and Indus Fan. Figs 2 and 3A inset show the difference between the modern trunk Indus which drains the Asian plate, arc and Indian plate, versus the modern Punjabi tributary system which drains, for the most part, only the Indian plate.

For the interpretations made from this upstream-downstream comparison to be valid, the rocks at the evaluated locations must be the products of the palaeo-Indus. Whilst all three repositories studied, the peripheral foreland basin, the Lower Indus Axial Basin, and the Indus Fan, show evidence of derivation from at least as far north as the KLIA since Eocene times, we acknowledge evidence for input from north of the Shyok suture zone can be equivocal (see sections 2.3.1, 2.3.3 and 2.3.4).

Below, we summarise the salient points regarding the upstream and downstream repositories that are relevant to the characteristics required to document the timing of conjoinment of the Punjabi tributary system with the trunk Indus River as described above. We discuss the Murree Formation which is anomalous at MHS, Muzzafarabad and Balakot, but not at Paras, separately in section 5.2.

5.1.1. Comparison of the upstream peripheral foreland basin material with the downstream repositories in terms of Sr-Nd data

Our data from the upstream (peripheral foreland basin) show that values have remained broadly constant from the start of our studied record in the early-Mid Eocene Kuldana Formation (Fig. 2A), until the late Miocene Nagri Formation, when values become a little more negative. εNd(0) values in the downstream repositories are similar to the upstream in the early Eocene. However, values in the downstream repositories become more negative compared to the upstream, by Mid Eocene in the Indus

570 Fan and around the Eocene-Oligocene boundary in the Lower Indus Axial Basin (Fig. 2B). This shift
571 indicates a greater input of material from the Indian plate Himalayan terrane at this time.

572 From the more negative εNd(0) values recorded below compared to above the confluence throughout
573 the Neogene, we interpret that the Punjabi tributary system has drained into the palaeo-Indus
574 throughout the Neogene, and that the present drainage configuration was therefore established during
575 the Paleogene.

576 The consistency of εNd values from the Eocene to the Neogene in the upstream repository, in contrast
577 to the shift to more negative values in the downstream repositories should reflect the time when the
578 Punjabi tributary system joined the trunk Indus River. However, the difference in the time of the
579 downstream shift, at the Eocene-Oligocene time in the Lower Indus axial basin delta deposits and in the
580 mid Eocene in the Indus Fan indicates that more research is required before we can pinpoint the exact
581 time that the tributary system joined the trunk Indus. Nevertheless, with available data we can conclude
582 that the tributaries joined in the trunk Indus at or before the start of the Oligocene (Fig 5).

583 *5.1.2. Comparison of the upstream peripheral foreland basin material with the downstream repositories*
584 *in terms of detrital zircon U-Pb data*

585 Although intraformational variability, lack of data from the Oligocene in the peripheral foreland basin,
586 and lack of data from the Eocene in the downstream repositories limits the comparison, the data are
587 consistent with the interpretations determined the Sm-Nd data, that the Punjabi tributary system joined
588 the trunk River Indus by Oligocene times (section 5.1.1, Fig 5): The proportion of 40-200 Ma arc-aged
589 grains remains high throughout the Miocene in the peripheral foreland basin, and these values are
590 higher compared to Oligocene-Pliocene values in both downstream repositories (Fig. 3A and C, Table 1).
591 Data from the Eocene peripheral foreland basin is highly variable. However, at least some samples have

592 a proportion of arc-aged grains similar to the proportions of the Neogene peripheral foreland basin,
593 consistent with the pattern shown in the Sm-Nd data.

594 SI Figure SI 3 illustrates the river's evolution well, particularly by comparison to the Lower Indus Axial
595 Basin. Downstream samples have a greater affinity to Indian plate rocks and the modern Indus at its
596 mouth at Thatta, compared to the upstream peripheral foreland basin rocks which have greater affinity
597 to the arc and Asian plate, and the modern day Indus at the range front at Attock.

598 The variation in zircon U-Pb age spectra, and also in εNa values, between the onshore and offshore
599 downstream palaeo-Indus, and between the Eastern and Western Indus Fan (SI Figs. S1 and S3) is
600 intriguing. It could be the result of a number of factors, for example differences in sample preparation
601 procedures between operators, downstream influence of hydraulics, or additional material contributing
602 downstream, for example.

603 ***5.2. Interpretation of the Murree Formation***

604 Compared to the other peripheral foreland basin sediments sampled, the Zircon U-Pb data show
605 significantly higher proportions of old grains in the Murree Formation at MHS, Kotli, and at Balakot and
606 Muzaffarabad in the HKS, but not at Paras north of Balakot (Fig. 3B, SI Fig S2, Table 1). Where
607 accompanying Sr-Nd data are available (MHS and Paras only), there is a corresponding change to more
608 negative ε_{Nd} values at MHS (Fig 2A), mirroring the change noted in the zircon data. This signature
609 indicates a higher proportion of material derived from the Indian plate (see also SI Fig S3). These
610 deposits may be interpreted as the palaeo-Jhelum Punjab tributary, which has a similar zircon U-Pb
611 spectrum to the Murree Formation (Fig. 3B), and a drainage basin consisting predominantly of the
612 Indian plate (Fig 1C). The spatial distribution of our analysed samples is consistent with this
613 interpretation: a Himalayan-derived palaeo-Jhelum type signature is prevalent in Murree Formation
614 samples at Muzaffarabad (Fig 1B) located on the modern day Jhelum River, at MHS downstream and ca

615 10 miles to the west of the modern Jhelum River, and at Kotli, downstream and 20 kms east of the
616 modern Jhelum river. It is also prevalent at Balakot, ca 15 miles upstream of the modern Jhelum River,
617 which we suggest could have been in the flood plain of the palaeo-Jhelum. 5 miles further north still,
618 near Paras, the signature is more arc-like and in this palaeo-drainage scenario, we propose lies outwith
619 the floodplain of the palaeo-Jhelum. We note that at Muzaffarabad only, through which the modern
620 Jhelum River flows, a palaeo-Jhelum type signature is also recorded, in some samples, in the underlying
621 Eocene Kuldana Formation. This may reflect the early initiation of this river, insufficiently large in its
622 early evolution to affect the downstream.

623 Alternatively, the anomalous signature from the Murree Formation compared to the rest of the
624 Cenozoic sediments in the peripheral foreland basin may reflect increased input from the Himalaya
625 attributable to a pulse of exhumation recorded in the Himalaya in the early Miocene (section 2.1.2). A
626 coeval change to greater input from the Indian plate is also recorded in the Indus Fan (Feng et al., 2021)
627 and Kirthar Ranges (Zhuang et al., 2015), supporting this interpretation. Further analyses from Murree
628 Formation samples distal to the Jhelum River should distinguish between these two alternative
629 hypotheses.

630 The difference in Murree signature compared to the rest of the foreland basin cannot be ascribed to
631 bias associated with grain size variation since the difference is reflected in both bulk rock Sr-Nd and
632 zircon proxies. Nor is there any reason to consider that a potential difference in the degree of diagenesis
633 caused the difference, since zircons are largely unaffected by this process.

634 ***5.3 What caused the change in the geochemical signature of the Indus Fan at 5-6 Ma?***

635 The more recently proposed alternatives to drainage reorganisation (Clift and Blusztajn, 2005) to
636 explain the geochemical shift in the Indus Fan at 5-6 Ma all involve tectonic explanations, namely
637 variations in exhumation of the hinterland terranes, although the extent to which increased exhumation

638 of the Lesser Himalaya versus Greater Himalaya versus Karakoram is responsible, is debated (Chirouze et
639 al 2015, Clift et al 2019, Zhou et al. 2022). Changes in monsoonal intensification are not thought to have
640 been a major influence (Clift et al., 2019, Zhou et al 2022).

641 To what extent do our data support a tectonic explanation? We focus on the peripheral foreland, which
642 should provide the most tectonically- influenced archive, above any downstream influence from the
643 Punjabi tributary system. We compare our data from the Nagri Formation (11-8.5 Ma; Table 1) to
644 modern day Indus data at the range front, this time period encompassing the 5-6 Ma date over which
645 the geochemical shift in the Indus Fan occurred.

646 The average εNd value of the two samples from the Nagri Formation is -9.65. No data are available for
647 the modern Indus at the range front. The spatially closest sample is from Besham, just south of the MCT
648 (Fig. 1C). This sample has a value of -10.7, and we would expect a more negative value by the time the
649 river had crossed to the range front, having flowed over more of the Greater Himalaya and most
650 negative Lesser Himalaya (Table 1). Thus, the shift to more negative εNd values between the Nagri
651 Formation and the estimated value for the range front in modern times I shows that variation in upland
652 tectonics over this time period could have resulted in the shift to more negative εNd values seen in the
653 Indus Fan over this time period.

654 Assignment of zircon U-Pb age populations to distinct provenances is challenging with respect to overlap
655 of the older Karakoram and Indian plate grains. Nevertheless, the 1500-2300 Ma population is typical of
656 the Lesser Himalaya. This population makes up 3% of the Nagri sample. There is no sample from the
657 modern Indus River at the range front. However, there is a sample from upstream at Attock (Fig. 1C).
658 This sample has an 11% contribution from the 1500-2300 Ma population, and we would predict a higher
659 proportion of that population after the river has flowed over a greater proportion of Indian plate
660 material. The shift to a higher proportion of zircons with ages indicative of Lesser Himalayan input

between the Nagri Formation and the modern day (Fig 3(, therefore supports our observations from the Sm-Nd data, that upstream variations in tectonics could have resulted in the geochemical shift in the Indus Fan.

There are no modern river mica $^{40}Ar/^{39}Ar$ data from the range front. Modern river $^{40}Ar/^{39}Ar$ mica data from the trunk Indus at its river mouth at Thatta shows Plio-Pleistocene grains (1-5 Ma) indicative of rapid exhumation (Clift et al., 2004). Recording of these young grains in the trunk river but not in the tributaries draining only the Indian plate or Indian plate plus Hindu Kush (Clift et al., 2004; Najman et al., 2009; Zhuang et al., 2018) is consistent with the viewpoints of, for example, Chirouze et al. (2015) and Clift et al. (2022) Clift et al (2022), that the Karakoram and/or the Nanga Parbat syntaxis supplied this young material. Lag times determined from mica data from the Neogene peripheral foreland basin sedimentary rocks show no clear indication of rapid exhumation of the micas' source region after 14-16 Ma (Fig. 4) although n values are small and therefore populations may have been missed. Therefore a period of rapid exhumation occurred sometime between Nagri Formation times and present day, consistent with the view that changing exhumation in the hinterland was responsible for the geochemical shift at 5 Ma in the Indus Fan.

6. Conclusions

When the lower Indus River broadly attained its current drainage configuration, in particular when the Punjab tributary system joined the main trunk river, is undocumented. Comparison of ε_{Nd} bulk rock data and detrital zircon U-Pb data from Cenozoic paleo-Indus sedimentary rocks both upstream and downstream of the confluence of the Indus with the Punjab tributary system shows that throughout the Neogene, greater proportions of Indian plate material are recorded in the downstream compared to the

upstream repositories. We therefore conclude that the Punjabi tributary system, which transports predominantly Indian plate detritus, had joined the trunk Indus River prior to the Neogene.

Whilst provenance indicators show that the proportion of Indian plate material remains constant from Eocene to Neogene in the palaeo-Indus repository upstream of the confluence, the proportion of Indian plate material increases in the downstream repositories, at the Eocene-Oligocene boundary in the palaeo-delta, and in the mid Eocene in the Indus Fan. More research is required to understand the reasons for this discrepancy in timing of the shift in the downstream repositories, but nevertheless we can conclude that the Punjabi tributary system joined the palaeo-Indus trunk river at or before the start of the Oligocene.

Acknowledgements

G.Z. acknowledges financial support of a Marie Curie Postdoctoral Fellowship under the Initial Training Network iTECC funded by the EU REA under the FP7 implementation of the Marie Curie Action, under grant agreement # 316966. Imran Khan helped with the sample collection. We thank Joe DiPietro for his detailed insights into the geology of Pakistan and Peng Zhou for sharing the geology map shown in Fig. 1C. This paper benefitted from input from two anonymous reviewers.

Figures

Figure 1: A: Map showing modern drainage of the Indus River with the Punjab tributary system, and the Indus Fan (black dotted line). Also shown are the onshore lower Indus (Kirthar and Sulaiman) and offshore IODP, ODP and DSDP locations of previously published data (Roddaz et al. 2011, Zhuang et al 2015, Clift et al. (2001), Clift and Blusztajn (2005), Clift et al. (2019) and Feng et al (2021). with which we compare our new upstream data. Black rectangle shows the location of Fig 1B. **B:** locations of new data (this study) and various towns and published sample sites discussed in text. MHS = Murree Hill Station;

HKS = Hazara-Kashmir Syntaxis. Samples with prefix KG96 or 99 are from Paras in the HKS, prefix MU96 are from Murree Hill Station, and prefix KMSr, CHSr, and NgSr are from Chinji village area. **C:** Drainage superimposed on regional geology (from Clift et al., 2019). ISZ = Indus Suture zone, SSZ = Shyok Suture Zone, MCT =Main Central Thrust, MBT=Main Boundary Thrust, MFT = Main Frontal Thrust.

Figure 2: ε_{Nd} values from the upstream peripheral foreland basin in Pakistan (A), and downstream Lower Indus axial basin and Indus Fan (B) through time. In A, numbers adjacent to squares refer to sample numbers to left. Asterisks indicate new data. Open squares for modern Indus River at Besham and Thatta; hexagons are from the modern Punjabi tributaries (data from Clift et al 2002, Alizai et al. 2011, Chirouze et al 2015). In B: diamonds – data from the Sulaiman and Kirthar regions of the Lower Indus axial basin (Roddaz et al, 2011, Zhuang et al 2015); circles – data from the Indus Fan from Clift et al. (2001), Clift and Blusztajn (2005), Clift et al. (2019), Zhou et al 2021, and Feng et al (2021). Questions marks next to three Mid Eocene samples represent uncertainties in age for those samples, as depicted in the original publication of Clift et al (2001). HKS = Hazara-Kashmir Syntaxis; MHS = Murree Hill Station. MDA = maximum depositional age as determined from detrital grain ages (sections 2.2.1, 4.2 and 4.3). Grey horizontal shading between plots A and B denote roughly equivalent time periods.

Figure 3: Detrital zircon U-Pb data shown as cumulative age distribution plots. **A**: Pakistan peripheral foreland basin data excluding Murree Formation data except our new data. Kuldana Fm samples are Early-Mid Eocene, Murree Formation samples are Early Miocene, Kamlial Fm is Early-Mid Miocene, Chinji Fm is Mid Miocene, Nagri Fm is Late Miocene (Table 1). A inset: modern river data comparing the Indus at the range front at Attock, with rivers of the Punjabi tributary system. **B:** all Murree Formation data, both new and published, with comparison to the Jhelum modern river data. Murree Formation is Early Miocene. **C:** comparison between peripheral foreland basin data and downstream Lower Indus axial basin data and (inset) Indus Fan data. Eocene peripheral foreland basin data are omitted from the

figure as there are no comparative data from the downstream repositories. HKS = Hazara-Kashmir Syntaxis, MHS = Murree Hill Station. All new data are asterisked. Samples with superscripts are published data, as follows: [1]Ding et al (2016), [2]Qasim et al (2018), [3]Awais et al (2021), [4]Zhuang et al (2015), [5]Clift et al (2002), , [6]Clift et al (2004), [7]Clift et al (2019), [8] (Zhou et al, 2021), [9]Feng et al (2021), [10]Alizai et al (2011).

Figure 4: Ar-Ar mica data plotted against depositional age for new (asterisked) and published samples. Note: [1]Published data from [1]Clift et al (2004) for modern Indus River data at Thatta, [2]published data from Najman et al (2003) for lower Chinji Formation, [3]published data from Najman et al (2003) for the Kamlial Fm, and [4]published data from Najman et al (2001) for the Murree Formation at HKS. Apart from the lower Chinji Formation sample, Chinji and Nagri Formation samples are not tied to the magnetostratigraphically dated section (Johnson et al 1985, section 2.2.1), and therefore the depositional age range of these samples is shown by the grey bars. Note that Murree Formation samples are plotted on the y axis at the age of their MDAs.

Figure 5: schematic figure showing expected and actual changes in provenance characteristics of sedimentary archives upstream and downstream of the confluence, at the time when the Punjabi tributary system joins the palaeo-Indus trunk river, superimposed on the modern geology. More detail on analytical values summarised in this figure can be found in Table 1. Abbreviations: Av – average, Z – zircon, Eoc – Eocene, KLIA – Kohistan-Ladakh Island Arc.

Tables

Table 1: comparison of provenance data from the peripheral foreland basin with those from the Lower Indus Axial Basin and Indus Fan. Source region signatures also provided. Note that three “Mid Eocene” data points from the Indus Fan are omitted as the age was noted as questionable in the original publication of Clift et al (2001).

*Compiled source region data from Ahmad et al. (2000); Bignold and Treloar (2003); Clift et al. (2019); DeCelles et al. (2004); DeCelles et al. (2016b); Deniel et al. (1987); Gehrels et al. (2011); Ji et al. (2009); Khan et al. (1997); Khan et al. (2004); Khan et al. (2009); Mahéo et al. (2009); Miller et al. (1999); Najman (2006); Pan et al. (2014); Richards et al. (2005); Robinson et al. (2001); Whittington et al. (1999); Zhang et al. (2004); Zhu et al. (2012); Zhuang et al. (2018), and additional references as listed in Fig S3b.

Supplementary information

Text S1: detailed analytical methodologies and sample information

Table S1: Sr-Nd bulk mudstone data.

Table S2: detrital zircon U-Pb data.

Table S3: White mica Ar-Ar analyses.

Figure SI 1: Sr-Nd mixture modelling of end members (A), and new (asterisked) and previously published bulk rock data from the peripheral and axial foreland basins in Pakistan, and the Indus Fan, plotted on to a sub-region of Fig A (B). Downstream published data: [1]Roddaz et al (2011), [2]Zhuang et al (2015), [3] Clift et al. (2001), Clift and Blusztajn (2005), Clift et al. (2019), Zhou et al 2021, and [4]Feng et al (2021). Means and one standard errors are calculated from compiled data points (same symbols with smaller sizes and transparency) (Zhuang et al., 2015 and references therein). HKS = Hazara-Kashmir Syntaxis; MHS = Murree Hill Station.

Figure SI 2a and b – KDEs for new and published zircon U-Pb data, at two different scales, 0-400 Ma and 0-500 Ma. New data are shown by asterisks. Published data: [1]Alizai et al (2011) , [2]Clift et al (2022), [3]Ding et al (2016), [4]Qasim et al (2018), [5]Awais et al (2021).

Figure SI 3: MDS plot showing zircon U-Pb data for our new samples (asterisked) from the peripheral foreland basin (this study, red crosses), compared to downstream published data from the Kirthar and Sulaiman ranges (purple crosses, sample prefixes SR and Z, data from Roddaz et al, 2011 and Zhuang et al. 2015) and Indus Fan (data from Clift et al. 2019, Zhou et al 2021, Feng et al, 2022), grey crosses for Western Fan, black crosses for Eastern Fan. Also shown are published data from the modern Indus River upstream at Attock and downstream at Thatta (blue crosses, see Fig 1 for location, from Alizai et al 2011 and Clift et al. 2022), and end member source signatures (black hexagons for Asian plate and arc , KLA = Kohistan-Ladakh Island arc, KK = Karakoram, HK = Hindu Kush, and red squares for Indian plate TH=Tethyan Himalaya, GH = Greater Himalaya, LH = Lesser Himalaya. References for compiled end member data are listed in Fig 3I 3b.

Fig SI 4a and b – KDEs for new and published mica Ar-Ar data from the peripheral foreland basin, Pakistan, at two different scales, 0-500 Ma and 0-100 Ma. New data are asterisked, published data is referenced on the plot.

References

Abbasi, I.A., Friend, P.F., 1989. Uplift and evolution of the Himalayan orogenic belts, as recorded in the foredeep molasse sediments. Zeitschrift für Geomorphologie NF Supplementband 76, 75-88.

Ahmad, T., Harris, N., Bickle, M., Chapman, H., Bunbury, J., Prince, C., 2000. Isotopic constraints on the structural relationships between the lesser Himalayan series and the high Himalayan crystalline series, Garhwal Himalaya. Geological Society of America Bulletin 112, 467-477.

Aitchison, J.C., Ali, J.R., Davis, A.M., 2007. When and where did India and Asia collide? Journal of Geophysical Research: Solid Earth (1978–2012) 112.

Alizai, A., Carter, A., Clift, P.D., VanLaningham, S., Williams, J.C., Kumar, R., 2011. Sediment provenance, reworking and transport processes in the Indus River by U–Pb dating of detrital zircon grains. Global and Planetary Change 76, 33-55.

Andò, S., Aharonovich, S., Hahn, A., George, S., Clift, P., Garzanti, E., 2020. Integrating heavy-mineral, geochemical and biomarker analyses of Plio-Pleistocene sandy and silty turbidites: a novel approach for provenance studies (Indus Fan, IODP Expedition 355). Geological Magazine 157, 929-938.

Argles, T., Foster, G., Whittington, A., Harris, N., George, M., 2003. Isotope studies reveal a complete Himalayan section in the Nanga Parbat syntaxis. Geology 31, 1109-1112.

Awais, M., Qasim, M., Tanoli, J.I., Ding, L., Sattar, M., Baig, M.S., Pervaiz, S., 2021. Detrital Zircon Provenance of the Cenozoic Sequence, Kotli, Northwestern Himalaya, Pakistan; Implications for India–Asia Collision. Minerals 11, 1399.
Baig, M.S., Munir, M.-u.-H., 2007. Foraminiferal biostratigraphy of Yadgar area, Muzaffarabad Azad Kashmir, Pakistan. Journal of Himalayan Earth Sciences 40.
Bernet, M., van der Beek, P., Pik, R., Huyghe, P., Mugnier, J.L., Labrin, E., Szulc, A., 2006. Miocene to Recent exhumation of the central Himalaya determined from combined detrital zircon fission‐track and U/Pb analysis of Siwalik sediments, western Nepal. Basin Research 18, 393-412.
Bhattacharya, G., Robinson, D.M., Wielicki, M.M., 2020. Detrital zircon provenance of the Indus Group, Ladakh, NW India: Implications for the timing of the India-Asia collision and other syn-orogenic processes. GSA Bulletin.
Bignold, S., Treloar, P., 2003. Northward subduction of the Indian Plate beneath the Kohistan island arc, Pakistan Himalaya: new evidence from isotopic data. Journal of the Geological Society 160, 377-384.
Bossart, P., Ottiger, R., 1989. Rocks of the Murree Formation in northern Pakistan: indicators of a descending foreland basin of late Paleocene to middle Eocene age. Eclogae Geologicae Helvetiae 82, 133-165.
Bouilhol, P., Jagoutz, O., Hanchar, J.M., Dudas, F.O., 2013. Dating the India–Eurasia collision through arc magmatic records. Earth and Planetary Science Letters 366, 163-175.
Burbank, D.W., Beck, R.A., Mulder, T., 1996. The Himalayan foreland basin. The Tectonic Evolution of Asia, Cambridge University Press, eds An Yin and Mark Harrison., 149-190.
Burbank, D.W., Tahirkheli, R.K., 1985. The magnetostratigraphy, fission-track dating, and stratigraphic evolution of the Peshawar intermontane basin, northern Pakistan. Geological Society of America Bulletin 96, 539-552.
Cerveny, P., Johnson, N., 1989. Tectonic and geomorphic implications of Siwalik Group. Tectonics of the Western Himalayas 232, 129.
Cerveny, P., Johnson, N., Tahirkheli, R., Bonis, N., 1989. Tectonic and geomorphic implications of Siwalik Group heavy minerals, Tectonics of western Himalayas. Geological Society of America Special Paper 232, 129-136.
Chirouze, F., Huyghe, P., Chauvel, C., van der Beek, P., Bernet, M., Mugnier, J.-L., 2015. Stable Drainage Pattern and Variable Exhumation in the Western Himalaya since the Middle Miocene. The Journal of Geology 123, 1-20.
Clift, P., Shimizu, N., Layne, G., Blusztajn, J., Gaedicke, C., Schlüter, H.-U., Clark, M., Amjad, S., 2001a. Development of the Indus Fan and its significance for the erosional history of the Western Himalaya and Karakoram. Geological Society of America Bulletin 113, 1039-1051.
Clift, P.D., Blusztajn, J., 2005. Reorganization of the western Himalayan river system after five million years ago. Nature 438, 1001-1003.
Clift, P.D., Campbell, I.H., Pringle, M.S., Carter, A., Zhang, X., Hodges, K.V., Khan, A.A., Allen, C.M., 2004. Thermochronology of the modern Indus River bedload: New insight into the controls on the marine stratigraphic record. Tectonics 23.
Clift, P.D., Carter, A., Jonell, T.N., 2014. U–Pb dating of detrital zircon grains in the Paleocene Stumpata Formation, Tethyan Himalaya, Zanskar, India. Journal of Asian Earth Sciences 82, 80-89.
Clift, P.D., Carter, A., Krol, M., Kirby, E., 2002a. Constraints on India-Eurasia collision in the Arabian Sea region taken from the Indus Group, Ladakh Himalaya, India. The tectonic and climatic evolution of the Arabian Sea region, 97.
Clift, P.D., Lee, J.I., Hildebrand, P., Shimizu, N., Layne, G.D., Blusztajn, J., Blum, J.D., Garzanti, E., Khan, A.A., 2002b. Nd and Pb isotope variability in the Indus River System: implications for sediment provenance and crustal heterogeneity in the Western Himalaya. Earth and Planetary Science Letters 200, 91-106.

Clift, P.D., Mark, C., Alizai, A., Khan, H., Jan, M.Q., 2022. Detrital U–Pb rutile and zircon data show Indus River sediment dominantly eroded from East Karakoram, not Nanga Parbat. Earth and Planetary Science Letters 600, 117873.

Clift, P.D., Shimizu, N., Layne, G., Blusztajn, J., 2001b. Tracing patterns of unroofing in the Early Himalaya through microprobe Pb isotope analysis of detrital K-feldspars in the Indus Molasse, India. Earth and Planetary Science Letters 188, 475-491.

Clift, P.D., Zhou, P., Stockli, D.F., Blusztajn, J., 2019. Regional Pliocene exhumation of the Lesser Himalaya in the Indus drainage. Solid Earth 10, 647-661.

Coward, M., Jan, Q., Rex, D., Tarney, J., Thirwall, M., 1984. Geology of the south Central Karakoram and Kohistan, The international Karakoram project. International conference, pp. 71-85.

DeCelles, P., Gehrels, G., Najman, Y., Martin, A., Carter, A., Garzanti, E., 2004. Detrital geochronology and geochemistry of Cretaceous–Early Miocene strata of Nepal: implications for timing and diachroneity of initial Himalayan orogenesis. Earth and Planetary Science Letters 227, 313-330.

DeCelles, P.G., Carrapa, B., Gehrels, G.E., Chakraborty, T., Ghosh, P., 2016a. Along‐strike continuity of structure, stratigraphy, and kinematic history in the Himalayan thrust belt: The view from Northeastern India. Tectonics 35, 2995-3027.

DeCelles, P.G., Castañeda, I.S., Carrapa, B., Liu, J., Quade, J., Leary, R., Zhang, L., 2016b. Oligocene‐Miocene Great Lakes in the India‐Asia Collision Zone. Basin Research.

DeCelles, P.G., Gehrels, G.E., Quade, J., Ojha, T., 1998. Eocene‐early Miocene foreland basin development and the history of Himalayan thrusting, western and central Nepal. Tectonics 17, 741-765.

Deniel, C., Vidal, P., Fernandez, A., Le Fort, P., Peucat, J.-J., 1987. Isotopic study of the Manaslu granite (Himalaya, Nepal): inferences on the age and source of Himalayan leucogranites. Contributions to Mineralogy and Petrology 96, 78-92.

Ding, H., Zhang, Z., Dong, X., Tian, Z., Xiang, H., Mu, H., Gou, Z., Shui, X., Li, W., Mao, L., 2016a. Early Eocene (c. 50 Ma) collision of the Indian and Asian continents: Constraints from the North Himalayan metamorphic rocks, southeastern Tibet. Earth and Planetary Science Letters 435, 64-73.

Ding, L., Qasim, M., Jadoon, I.A., Khan, M.A., Xu, Q., Cai, F., Wang, H., Baral, U., Yue, Y., 2016b. The India–Asia collision in north Pakistan: Insight from the U–Pb detrital zircon provenance of Cenozoic foreland basin. Earth and Planetary Science Letters 455, 49-61.

DiPietro, J., Hussain, A., Ahmad, I., Khan, M.A., 2000. The main mantle thrust in Pakistan: its character and extent. Geological Society, London, Special Publications 170, 375-393.

DiPietro, J.A., Ahmad, I., Hussain, A., 2008. Cenozoic kinematic history of the Kohistan fault in the Pakistan Himalaya. Geological Society of America Bulletin 120, 1428-1440.

DiPietro, J.A., Pogue, K.R., 2004. Tectonostratigraphic subdivisions of the Himalaya: A view from the west. Tectonics 23.

DiPietro, J.A., Pullen, A., Krol, M.A., 2021. Geologic history and thermal evolution in the hinterland region, western Himalaya, Pakistan. Earth-Science Reviews 223, 103817.

Dunlap, W.J., Weinberg, R.F., Searle, M.P., 1998. Karakoram fault zone rocks cool in two phases. Journal of the Geological Society 155, 903-912.

Exnicios, E.M., Carter, A., Najman, Y., Clift, P.D., 2022. Late Miocene unroofing of the Inner Lesser Himalaya recorded in the NW Himalaya foreland basin. Basin Research 34, 1894-1916.

Feng, H., Lu, H., Carrapa, B., Zhang, H., Chen, J., Wang, Y., Clift, P.D., 2021. Erosion of the Himalaya-Karakoram recorded by Indus Fan deposits since the Oligocene. Geology.

Fraser, J.E., Searle, M.P., Parrish, R.R., Noble, S.R., 2001. Chronology of deformation, metamorphism, and magmatism in the southern Karakoram Mountains. Geological Society of America Bulletin 113, 1443-1455.

Gaetani, M., Garzanti, E., 1991. Multicyclic history of the Northern India continental margin (Northwestern Himalaya)(1). AAPG Bulletin 75, 1427-1446.

Gaetani, M., Jadoul, F., Erba, E., Garzanti, E., 1993. Jurassic and Cretaceous orogenic events in the North Karakoram: age constraints from sedimentary rocks. Geological Society, London, Special Publications 74, 39-52.
Garzanti, E., Andò, S., 2019. Heavy minerals for junior woodchucks. Minerals 9, 148.
Garzanti, E., Andò, S., Vezzoli, G., 2009. Grain-size dependence of sediment composition and environmental bias in provenance studies. Earth and Planetary Science Letters 277, 422-432.
Garzanti, E., Andò, S., Vezzoli, G., 2020. Provenance of cenozoic indus fan sediments (IODP Sites U1456 and U1457). Journal of Sedimentary Research 90, 1114-1127.
Gehrels, G., Kapp, P., DeCelles, P., Pullen, A., Blakey, R., Weislogel, A., Ding, L., Guynn, J., Martin, A., McQuarrie, N., 2011. Detrital zircon geochronology of pre‐Tertiary strata in the Tibetan‐Himalayan orogen. Tectonics 30.
Henderson, A.L., Najman, Y., Parrish, R., BouDagher‐Fadel, M., Barford, D., Garzanti, E., Andò, S., 2010. Geology of the Cenozoic Indus Basin sedimentary rocks: Paleoenvironmental interpretation of sedimentation from the western Himalaya during the early phases of India‐Eurasia collision. Tectonics 29.
Henderson, A.L., Najman, Y., Parrish, R., Mark, D.F., Foster, G.L., 2011. Constraints to the timing of India–Eurasia collision; a re-evaluation of evidence from the Indus Basin sedimentary rocks of the Indus–Tsangpo Suture Zone, Ladakh, India. Earth-Science Reviews 106, 265-292.
Hildebrand, P., Noble, S., Searle, M., Parrish, R., 1998. Tectonic significance of 24 Ma crustal melting in the eastern Hindu Kush, Pakistan. Geology 26, 871-874.
Hildebrand, P., Noble, S., Searle, M., Waters, D., Parrish, R., 2001. Old origin for an active mountain range: Geology and geochronology of the eastern Hindu Kush, Pakistan. Geological Society of America Bulletin 113, 625-639.
Hodges, K.V., 2000. Tectonics of the Himalaya and southern Tibet from two perspectives. Geological Society of America Bulletin 112, 324-350.
Hu, X., Garzanti, E., Wang, J., Huang, W., An, W., Webb, A., 2016. The timing of India-Asia collision onset–Facts, theories, controversies. Earth-Science Reviews 160, 264-299.
Ji, W., Wu, F., Liu, C., Chung, S., 2009. Geochronology and petrogenesis of granitic rocks in Gangdese batholith, southern Tibet. Science in China Series D: Earth Sciences 52, 1240-1261.
Johnson, N.M., Stix, J., Tauxe, L., Cerveny, P.F., Tahirkheli, R.A., 1985. Paleomagnetic chronology, fluvial processes, and tectonic implications of the Siwalik deposits near Chinji Village, Pakistan. The Journal of Geology, 27-40.
Jonell, T.N., Li, Y., Blusztajn, J., Giosan, L., Clift, P.D., 2018. Signal or noise? Isolating grain size effects on Nd and Sr isotope variability in Indus delta sediment provenance. Chemical Geology 485, 56-73.
Khan, M.A., STERN, R.J., GRIBBLE, R.F., WINDLEY, B.F., 1997. Geochemical and isotopic constraints on subduction polarity, magma sources, and palaeogeography of the Kohistan intra-oceanic arc, northern Pakistan Himalaya. Journal of the Geological Society 154, 935-946.
Khan, S., Stern, R., Manton, M., Copeland, P., Kimura, J., Khan, M., 2004. Age, geochemical and Sr–Nd–Pb isotopic constraints for mantle source characteristics and petrogenesis of Teru Volcanics, Northern Kohistan Terrane, Pakistan. Tectonophysics 393, 263-280.
Khan, S.D., Walker, D.J., Hall, S.A., Burke, K.C., Shah, M.T., Stockli, L., 2009. Did the Kohistan-Ladakh island arc collide first with India? Geological Society of America Bulletin 121, 366-384.
Koppers, A.A., 2002. ArArCALC—software for 40 Ar/39 Ar age calculations. Computers & Geosciences 28, 605-619.
Leier, A.L., Kapp, P., Gehrels, G.E., DeCelles, P.G., 2007. Detrital zircon geochronology of Carboniferous–Cretaceous strata in the Lhasa terrane, Southern Tibet. Basin Research 19, 361-378.

Mahéo, G., Blichert-Toft, J., Pin, C., Guillot, S., Pêcher, A., 2009. Partial melting of mantle and crustal sources beneath South Karakorum, Pakistan: implications for the Miocene geodynamic evolution of the India–Asia convergence zone. Journal of Petrology 50, 427-449.
Malusà, M.G., Resentini, A., Garzanti, E., 2016. Hydraulic sorting and mineral fertility bias in detrital geochronology. Gondwana Research 31, 1-19.
Miller, C., Schuster, R., Klötzli, U., Frank, W., Purtscheller, F., 1999. Post-collisional potassic and ultrapotassic magmatism in SW Tibet: geochemical and Sr–Nd–Pb–O isotopic constraints for mantle source characteristics and petrogenesis. Journal of Petrology 40, 1399-1424.
Najman, Y., 2006. The detrital record of orogenesis: A review of approaches and techniques used in the Himalayan sedimentary basins. Earth-Science Reviews 74, 1-72.
Najman, Y., Bickle, M., Garzanti, E., Pringle, M., Barfod, D., Brozovic, N., Burbank, D., Ando, S., 2009. Reconstructing the exhumation history of the Lesser Himalaya, NW India, from a multitechnique provenance study of the foreland basin Siwalik Group. Tectonics 28.
Najman, Y., Garzanti, E., Pringle, M., Bickle, M., Stix, J., Khan, I., 2003. Early-Middle Miocene paleodrainage and tectonics in the Pakistan Himalaya. Geological Society of America Bulletin 115, 1265-1277.
Najman, Y., Pringle, M., Godin, L., Oliver, G., 2001. Dating of the oldest continental sediments from the Himalayan foreland basin. Nature 410, 194-197.
Najman, Y., Pringle, M., Godin, L., Oliver, G., 2002. A reinterpretation of the Balakot Formation: Implications for the tectonics of the NW Himalaya, Pakistan. Tectonics 21, 9-1-9-18.
Nyberg, B., Helland-Hansen, W., Gawthorpe, R.L., Sandbakken, P., Eide, C.H., Sømme, T., Hadler-Jacobsen, F., Leiknes, S., 2018. Revisiting morphological relationships of modern source-to-sink segments as a first-order approach to scale ancient sedimentary systems. Sedimentary Geology 373, 111-133.
Palin, R., Searle, M., Waters, D., Horstwood, M., Parrish, R., 2012. Combined thermobarometry and geochronology of peraluminous metapelites from the Karakoram metamorphic complex, North Pakistan; New insight into the tectonothermal evolution of the Baltoro and Hunza Valley regions. Journal of Metamorphic Geology 30, 793-820.
Pan, F.-B., Zhang, H.-F., Xu, W.-C., Guo, L., Wang, S., Luo, B.-j., 2014. U–Pb zircon chronology, geochemical and Sr–Nd isotopic composition of Mesozoic–Cenozoic granitoids in the SE Lhasa terrane: Petrogenesis and tectonic implications. Lithos 192, 142-157.
Pivnik, D.A., Wells, N.A., 1996. The transition from Tethys to the Himalaya as recorded in northwest Pakistan. Geological Society of America Bulletin 108, 1295-1313.
Qasim, M., Ding, L., Khan, M.A., Jadoon, I.A., Haneef, M., Baral, U., Cai, F., Wang, H., Yue, Y., 2018. Tectonic implications of detrital zircon ages from lesser Himalayan Mesozoic - Cenozoic strata, Pakistan. Geochemistry, Geophysics, Geosystems 19, 1636-1659.
Qayyum, M., Niem, A.R., Lawrence, R.D., 2001. Detrital modes and provenance of the Paleogene Khojak Formation in Pakistan: Implications for early Himalayan orogeny and unroofing. Geological Society of America Bulletin 113, 320-332.
Richards, A., Argles, T., Harris, N., Parrish, R., Ahmad, T., Darbyshire, F., Draganits, E., 2005. Himalayan architecture constrained by isotopic tracers from clastic sediments. Earth and Planetary Science Letters 236, 773-796.
Robinson, D.M., DeCelles, P.G., Patchett, P.J., Garzione, C.N., 2001. The kinematic evolution of the Nepalese Himalaya interpreted from Nd isotopes. Earth and Planetary Science Letters 192, 507-521.
Roddaz, M., Said, A., Guillot, S., Antoine, P.-O., Montel, J.-M., Martin, F., Darrozes, J., 2011. Provenance of Cenozoic sedimentary rocks from the Sulaiman fold and thrust belt, Pakistan: implications for the palaeogeography of the Indus drainage system. Journal of the Geological Society 168, 499-516.

Schaltegger, U., Zeilinger, G., Frank, M., Burg, J.P., 2002. Multiple mantle sources during island arc magmatism: U–Pb and Hf isotopic evidence from the Kohistan arc complex, Pakistan. Terra Nova 14, 461-468.
Schärer, U., Hamet, J., Allègre, C.J., 1984. The Transhimalaya (Gangdese) plutonism in the Ladakh region: a U Pb and Rb Sr study. Earth and Planetary Science Letters 67, 327-339.
Schneider, D., Zeitler, P., Kidd, W., Edwards, M., 2001. Geochronologic constraints on the tectonic evolution and exhumation of Nanga Parbat, western Himalaya syntaxis, revisited. The Journal of Geology 109, 563-583.
Searle, M., Khan, M.A., Fraser, J., Gough, S., Jan, M.Q., 1999. The tectonic evolution of the Kohistan‐Karakoram collision belt along the Karakoram Highway transect, north Pakistan. Tectonics 18, 929-949.
Searle, M., Parrish, R.R., Thow, A., Noble, S., Phillips, R., Waters, D., 2010. Anatomy, age and evolution of a collisional mountain belt: the Baltoro granite batholith and Karakoram Metamorphic Complex, Pakistani Karakoram. Journal of the Geological Society 167, 183-202.
Shah, S.I., 2009. Stratigraphy of Pakistan. Government of Pakistan Ministry of Petroleum & Natural Resorces Geological Survey of Pakistan.
Sinclair, H., Jaffey, N., 2001. Sedimentology of the Indus Group, Ladakh, northern India: implications for the timing of initiation of the palaeo-Indus River. Journal of the Geological Society 158, 151-162.
Treloar, P., Rex, D., Guise, P., Wheeler, J., Hurford, A., Carter, A., 2000. Geochronological constraints on the evolution of the Nanga Parbat syntaxis, Pakistan Himalaya. Geological Society, London, Special Publications 170, 137-162.
Treloar, P.J., Palin, R.M., Searle, M.P., 2019. Towards resolving the metamorphic enigma of the Indian Plate in the NW Himalaya of Pakistan. Geological Society, London, Special Publications 483, 255-279.
Ullah, K., Arif, M., Shah, M.T., 2015. Geochemistry and provenance of the Lower Siwaliks from southwestern Kohat, western Himalayan Foreland Basin, NW Pakistan. Geologica Acta: an international earth science journal 13, 45-61.
Van Der Beek, P., Van Melle, J., Guillot, S., Pêcher, A., Reiners, P.W., Nicolescu, S., Latif, M., 2009. Eocene Tibetan plateau remnants preserved in the northwest Himalaya. Nature Geoscience 2, 364-368.
van Hinsbergen, D.J., Lippert, P.C., Dupont-Nivet, G., McQuarrie, N., Doubrovine, P.V., Spakman, W., Torsvik, T.H., 2012. Greater India Basin hypothesis and a two-stage Cenozoic collision between India and Asia. Proceedings of the National Academy of Sciences 109, 7659-7664.
Wallis, D., Carter, A., Phillips, R.J., Parsons, A.J., Searle, M.P., 2016. Spatial variation in exhumation rates across Ladakh and the Karakoram: New apatite fission track data from the Eastern Karakoram, NW India. Tectonics.
Welcomme, J.-L., Benammi, M., Crochet, J.-Y., Marivaux, L., Métais, G., Antoine, P.-O., Baloch, I., 2001. Himalayan Forelands: palaeontological evidence for Oligocene detrital deposits in the Bugti Hills (Balochistan, Pakistan). Geological Magazine 138, 397-405.
Whittington, A., Foster, G., Harris, N., Vance, D., Ayres, M., 1999. Lithostratigraphic correlations in the western Himalaya—an isotopic approach. Geology 27, 585-588.
Willis, B., 1993. Evolution of Miocene fluvial systems in the Himalayan foredeep through a two kilometer-thick succession in northern Pakistan. Sedimentary geology 88, 77-121.
Yeats, R.S., Hussain, A., 1987. Timing of structural events in the Himalayan foothills of northwestern Pakistan. Geological society of America bulletin 99, 161-176.
Yu, Z., Colin, C., Wan, S., Saraswat, R., Song, L., Xu, Z., Clift, P., Lu, H., Lyle, M., Kulhanek, D., 2019. Sea level-controlled sediment transport to the eastern Arabian Sea over the past 600 kyr: Clay minerals and SrNd isotopic evidence from IODP site U1457. Quaternary Science Reviews 205, 22-34.
Zaleha, M.J., 1997. Intra‐and extrabasinal controls on fluvial deposition in the Miocene Indo‐Gangetic foreland basin, northern Pakistan. Sedimentology 44, 369-390.

Zanchi, A., Gaetani, M., 2011. The geology of the Karakoram range, Pakistan: the new 1: 100,000 geological map of Central-Western Karakoram. Italian journal of geosciences 130, 161-262.
Zhang, H., Harris, N., Parrish, R., Kelley, S., Zhang, L., Rogers, N., Argles, T., King, J., 2004. Causes and consequences of protracted melting of the mid-crust exposed in the North Himalayan antiform. Earth and Planetary Science Letters 228, 195-212.
Zhou, P., Stockli, D.F., Ireland, T., Murray, R.W., Clift, P.D., 2021. Zircon U‐Pb Age Constraints on NW Himalayan Exhumation from the Laxmi Basin, Arabian Sea. Geochemistry, Geophysics, Geosystems, e2021GC010158.
Zhou, P., Stockli, D.F., Ireland, T., Murray, R.W., Clift, P.D., 2022. Zircon U‐Pb Age Constraints on NW Himalayan Exhumation from the Laxmi Basin, Arabian Sea. Geochemistry, Geophysics, Geosystems, e2021GC010158.
Zhu, D.-C., Mo, X.-X., Niu, Y., Zhao, Z.-D., Wang, L.-Q., Liu, Y.-S., Wu, F.-Y., 2009. Geochemical investigation of Early Cretaceous igneous rocks along an east–west traverse throughout the central Lhasa Terrane, Tibet. Chemical Geology 268, 298-312.
Zhu, D.-C., Zhao, Z.-D., Niu, Y., Dilek, Y., Wang, Q., Ji, W.-H., Dong, G.-C., Sui, Q.-L., Liu, Y.-S., Yuan, H.-L., 2012. Cambrian bimodal volcanism in the Lhasa Terrane, southern Tibet: record of an early Paleozoic Andean-type magmatic arc in the Australian proto-Tethyan margin. Chemical Geology 328, 290-308.
Zhuang, G., Najman, Y., Guillot, S., Roddaz, M., Antoine, P.-O., Métais, G., Carter, A., Marivaux, L., Solangi, S.H., 2015. Constraints on the collision and the pre-collision tectonic configuration between India and Asia from detrital geochronology, thermochronology, and geochemistry studies in the lower Indus basin, Pakistan. Earth and Planetary Science Letters 432, 363-373.
Zhuang, G., Najman, Y., Tian, Y., Carter, A., Gemignani, L., Wijbrans, J., Jan, M.Q., Khan, M.A., 2018. Insights into the evolution of The Hindu Kush-Kohistan-Karakoram from modern river sand detrital geo- and thermochronological studies. Journal of the Geological Society, jgs2018-2007.

Terrane/ Basin Stratigraphy	εNd	Zircons % with U-Pb ages 40-200 Ma (arc-derived)
Source region characteristics* (GHS, LHS, THS = Greater-, Lesser-, Tethyan Himalaya respectively; NP = Nanga Parbat)		
Karakoram	Average: -10	Dominant 40-200 Ma populations with some older grains to Precambrian
Kohistan Island arc	Average: +5	Entirely 40-200 Ma
Indian plate	Avgs: -15 (GHS), -22 (LHS & NP), -11 (THS)	Near 100% > 200 Ma.
Upstream peripheral foreland basin (new & published data of [1]Clift et al 2002, [2]Alizai et al., 2011 and Clift et al 2022, [3]Ding et al 2016, [4]Qasim et al 2018)		
Modern Indus River	*No data for downstream of GHS* [1]At Skardu (upstream of GHS) -8.6 [1]At Besham (just into GHS) -10.7	[2]At Attock: 53% arc
Upper Miocene Nagri Fm	-9.4, -9.9	67% arc
Mid Miocene Chinji Fm	-7.7, -8.7 (our data). Chirouze et al., (2015) data: -3.8 to -7.7	47% arc
L-mid Miocene Kamlial Fm	-8.3	51% arc
Lower Miocene Murree Fm	-13.8 (MHS) -8.1, -9.2 (HKS, Paras north of Balakot)	23% arc (MHS) 50% arc (HKS, Paras north of Balakot) [3]0-4% arc (HKS, Balakot) [3]0-17% (HKS Muzaffarabad)
Lower-mid Eocene Kuldana Fm	-8.1, -8.8	[3]49-75% arc (HKS, Balakot) [3]6-74% arc (HKS, Muzaffarabad) Qasim Murree Hill station [4]34-78% arc (MHS)
Downstream Lower Indus axial basin, Kirthar (K) and Sulaiman (S) regions ([1]Clift et al. 2002, [5]Clift et al. 2004, [6]Roddaz et al 2011, [7]Zhuang et al. 2015)		
Modern Indus River	-15[1] (below Sutlej confluence and at delta)	[5]At Thatta: 18% arc
Pliocene Siwalik Gp	-12 ([7]K) n=2	12% arc ([7]K)
U. Miocene Siwaliks	-9.3 ([7]K) n=1	
M. Miocene Siwalik Gp & Vihowa Fm	-11 ([7]K) n=8	22% arc ([7]K)
L. Miocene Vihowa & Chitarwata Fms.	-10.5 ([6]S) n=2, -13.1 ([7]K) n=5	
Upper Oligocene Chitarwata Fm	Upper upper Oligocene -11.1 ([6]S) n=3 Lower upper Oligocene -12.4 ([6]S) n=3	
Lower Oligocene Chitarwata Fm	-9.6 ([6]S) n=1; -13.4 ([7]K) n=1	16% arc ([7]K); 16% arc ([7]S)
L-mid Eocene Ghazij & Kirthar Gps	Av.-9.3 ([6]S) n=2, -7.5 ([7]K) n=1	
Indus Fan ([8]Clift et al 2001 ; [9]Clift & Blusztajn 2005; [10]Clift et al 2019 ; [11]Feng et al. 2021 ; [12]Zhou et al. 2022).		
Pliocene	[9]Av. -10.8 (n=8)	[10, 12]19-32%
Miocene	[8,10,11]Av. -10.1 (n=47)	[10,11, 12]11-48%
Oligocene	[8, 10]Av. -11.9 (n=16)	[11]16-43%
M. Eocene	[8]-11.96, -5.2	
E. Eocene	[9]-9.3	

Figure 1A map

60°
70°
80°
40°
30°
20°
Tarim
Pamir
Transverse
Upper Indus
Axial Upper Indus
HKS
KP
PP
Tibetan
Plateau
Katawaz
Himalayas
Sulaiman
Ranges
Punjab
(Himalayan)
tributaries
Lower
Indus
basin
Kirthar
Ranges
Study locations
In Sulaiman
In Kirthar
PP: Potwar Plateau
HKS: Hazara-Kashmir Syntaxis
KP: Kohat Plateau
Dotted line: Indus fan
Arabian Sea
ODP 731
Indus Fan
IODP U1457
DSDP 224
ODP 720
IODP U1456
–5000
0
5000
Topography (m)

Figure 1 b c

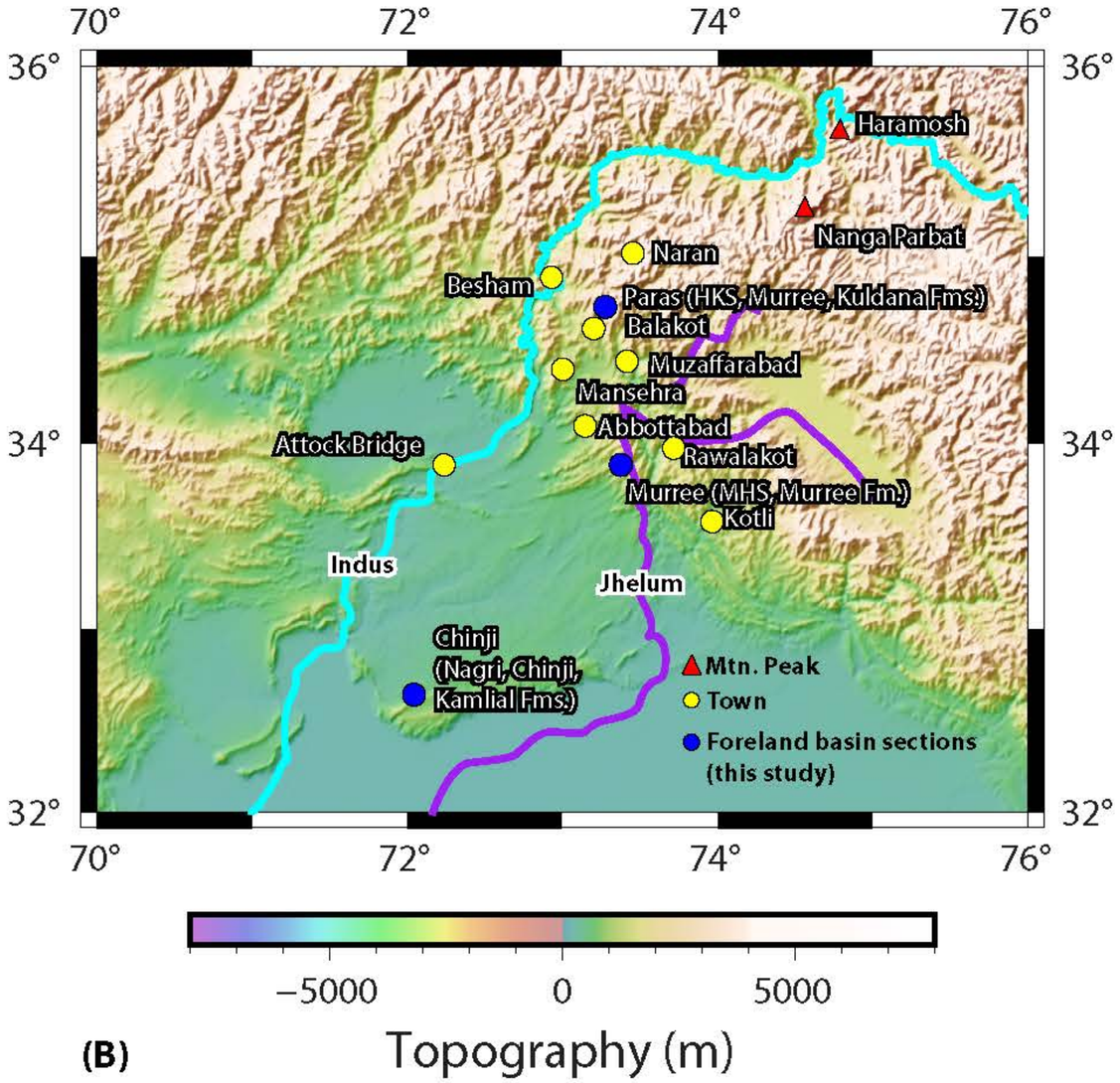

(B)

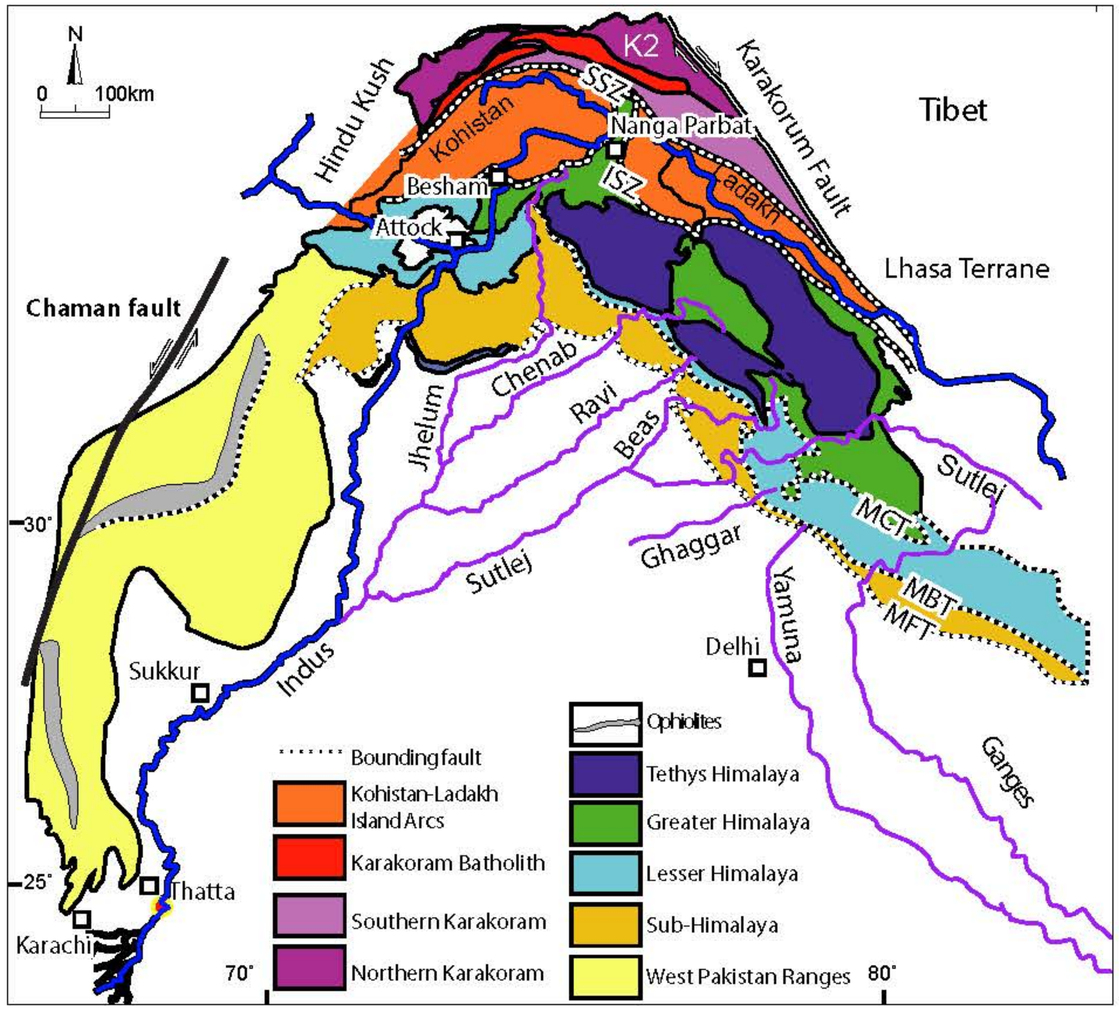

(C)

Figure 2 eps Nd against stratigraphy

(A)

modern river sediments

Indus at Thatta

Indus at Besham

Sutlej Jhelum Chenab Ravi

First stratigraphic samples mean (n = 9; this study, excluding the Murree Fm at MHS)

Age (Ma)

1 - NGSr-1A (Nagri Fm) *
2 - NGSr-2A (Nagri Fm) *
3 - CHSr-2A (Chinji Fm) *
4 - CHSr-1A (Chinji Fm) *
5 - KMSr-5A (Kamlial Fm) *
6 - MU96-2C (Murree Fm at MHS) *
7 - KG96-22C (Murree Fm at HKS) *
8 - KG96-30A (Murree Fm at HKS) *
9 - KG99-5E (Kuldana Fm) *
10 - KG99-14C (Kuldana Fm) *

11-8.5 Ma
14-11 Ma
18-14 Ma
MDA (MHS): 24 Ma
MDA (HKS): 23 Ma
53-43 Ma

1 2 4 3 5 6 8 7 9 10

(?) (?) (?)

0 10 20 30 40 50

-20 -15 -10 -5

-15 -10 -5

ε_{Nd} ε_{Nd}

Figure 3 Zircon U-Pb cumulative plot

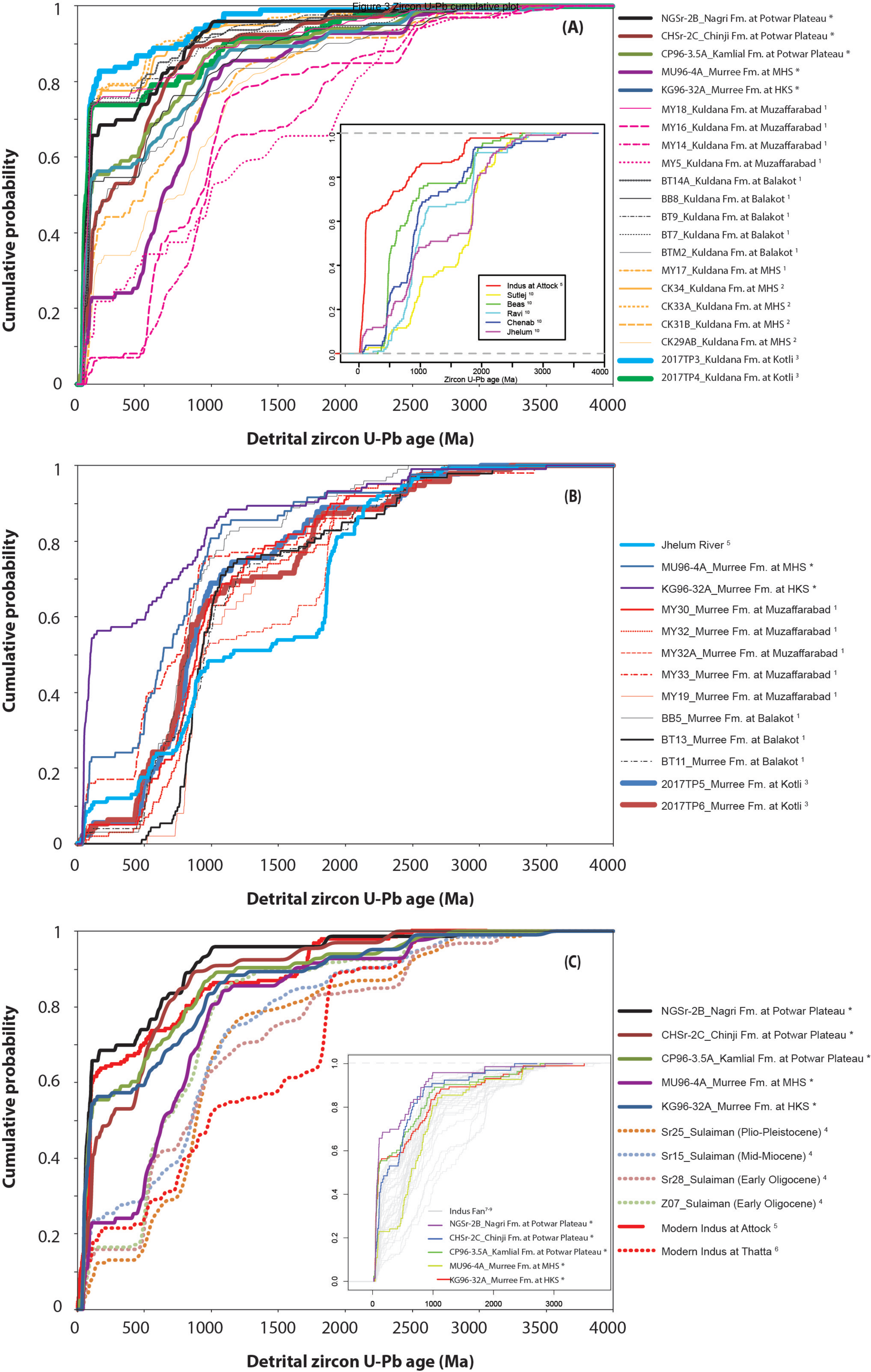

Figure 4 mica Ar-Ar lag time plot

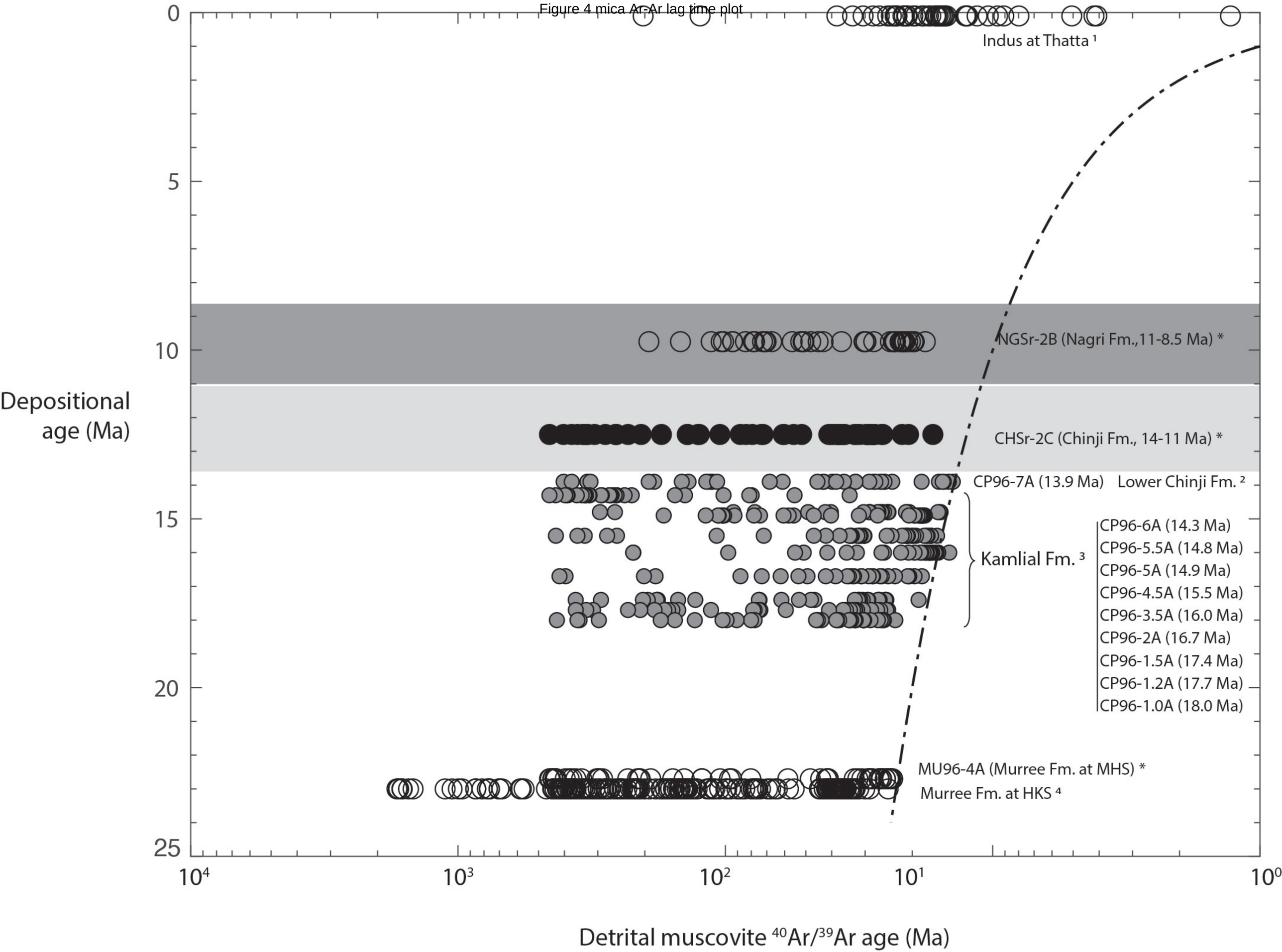

Figure 5 schematic palaeodrainage